

Overall, the paper presents interesting findings. However, a more detailed description of the physical processes leading to eg the gradient in GCR flux would improve the scientific content significantly.

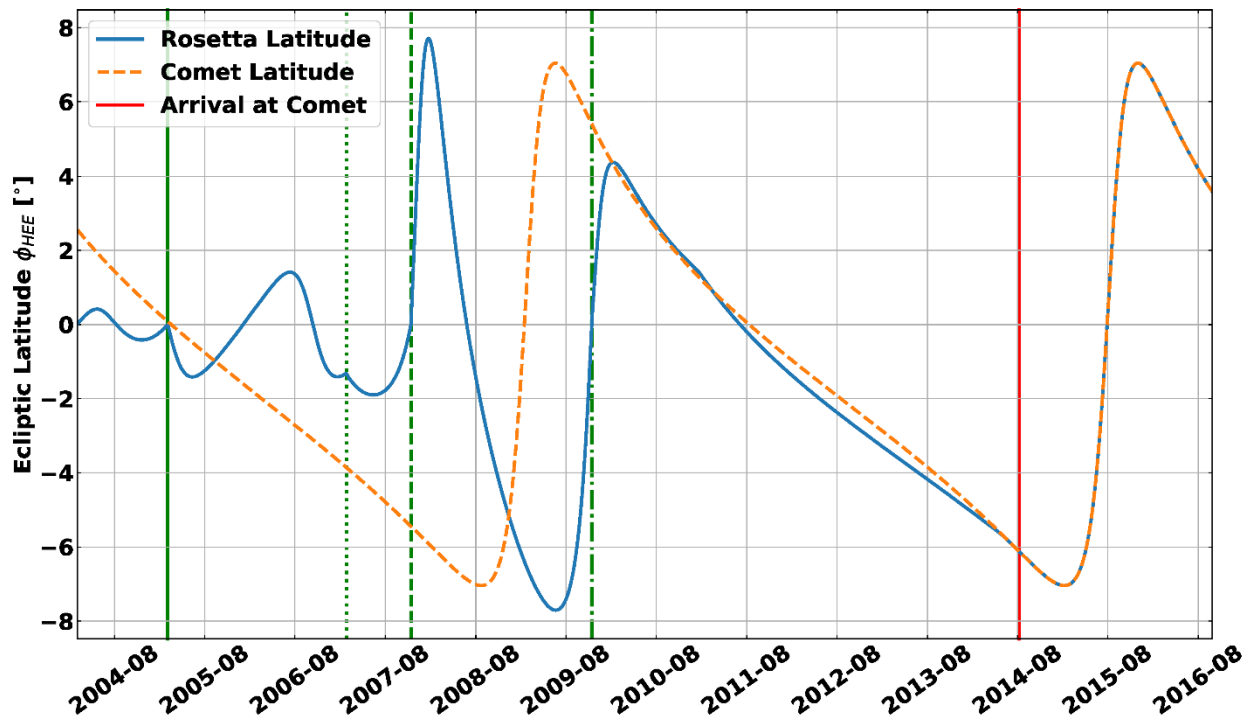
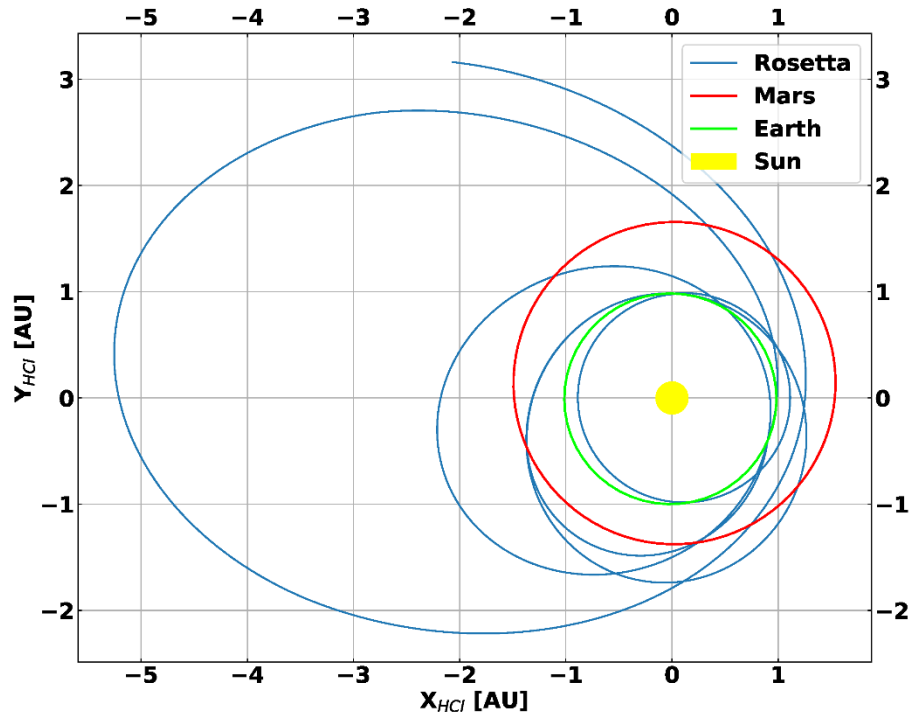
We thank Charlotte Goetz for her feedback.

We plan to update the introduction in the revised article. The following the sentence “The variation of GCRs as a function of different factors (solar cycle, heliocentric distance, solar wind conditions) is an interesting topic to explore, and lead to a better understanding of the heliosphere”is replaced by:

“The variation in galactic cosmic rays intensity depends on different physical processes: inward diffusion in the interplanetary magnetic field, adiabatic cooling, outward convection and deceleration in the solar wind plasma, drift along the heliospheric current sheet, and interaction with magnetic structures in shocks and in interplanetary coronal mass ejections (e.g. McKibben; Potgieter, 2013; Morral 2013; Alania et al., 2014; Kozai et al. 2014; Giseler and Heber 2016). The GCR intensity is therefore varying with the solar wind velocity, the magnitude of the interplanetary magnetic field, solar activity, the heliospheric current sheet tilt angle, and the solar polarity change.”

Figure 1a: the green and blue are hard to distinguish, maybe another color combination would be better here.

The figure was updated. See below.

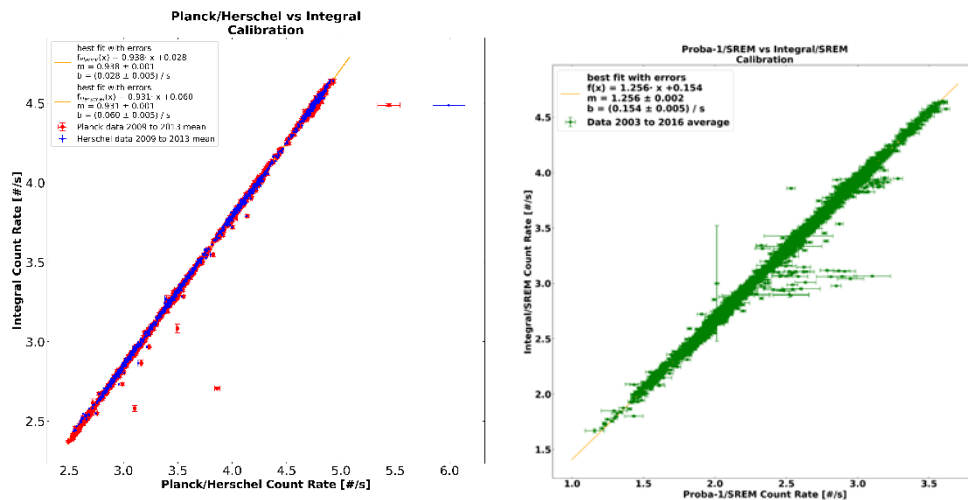


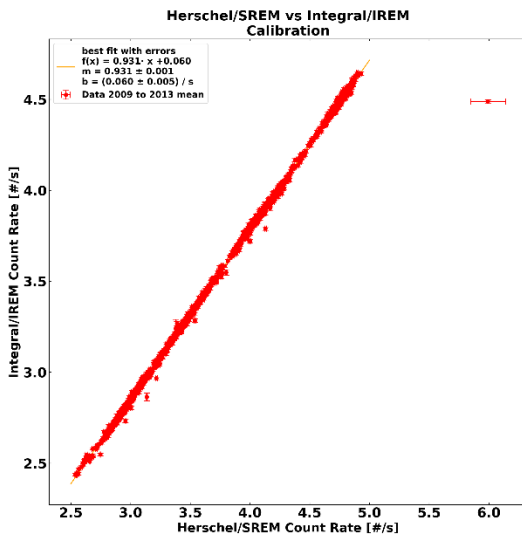
1. It is unclear to me why the instruments need cross-calibration. What are the technical reasons for the instruments different behaviour if they are essentially the same model? You mention sensitivity area, can you elaborate further? Do you have any reason to believe that the dependence of the countrate of two instruments is linear? Could it also be something else? (second or third order?)

Even if the radiation monitors are of the same design, they are not identical copies. It is therefore reasonable to assume that they will have similar performances, but not equal. In fact, the purpose of the cross-calibration is:

- Show that the radiation monitor family behave similarly. This is a good engineering achievement, useful to report.
- The response of a particle detector also depends on the radiation environment it is exposed to. In this case, SREM detectors are mounted on/within spacecraft, which may generate secondary particles that modify the radiation environment at the detector to be different from that in deep space. Therefore, the instrument cross-calibration would help to reduce the related uncertainties.
- Normalise the count rate in case quantitative cross-mission studies are performed, like in the present article.

In the article, we do not elaborate further regarding the linearity of the calibration. Second or higher orders are always possible, but looking at the behaviour (like see the plots below for Herschel, Planck, INTEGRAL and Proba-1 monitors), a linear fit appears to us very reasonable to consider.





2. p713: the equation given here is not consistent with what is shown in Figure 2. From figure two the relationship should actually be: $\text{Count}(\text{Integral}) = 1.028 \times \text{count}(\text{Rosetta}) - 0.127$. Then all the other calibration functions should also be checked.

The relationship is correct: $\text{Integral} = 1.028 \text{ Rosetta} - 0.12$. The text was corrected.

3. p11I21ff: The correlation is very obvious. You say this is something that was expected and address this briefly in the annex. I think it would be better suited here and needs to be explained in more scientific detail.

Page 12, we add the following sentence: "This anticorrelation is due to the modulation of GCR intensity. The GCR intensity decreases when the magnetic field and the solar activity increase due to the GCR diffusion in the solar wind. This "engineering" data is a new data set that can be useful to study this modulation.", after "In addition, the expected anticorrelation between GCR and IMF and Sun spot number was calculated and the result can be found in Annex 1."

4. p12I11ff: Again, a physical explanation of why this gradient is expected would be good.

This was added. It is here only a question of heliocentric distance. GCRs propagate in the solar system, and their flux decrease with the solar distance, due to the increasing strength of the magnetic field.

New sentence: This positive gradient is mainly due to the inward diffusion of GCRs in an interplanetary magnetic field whose strength decreases with heliocentric distance.

5. p15I22: However, they ARE highly.....

6. p15I31: demonstrate → demonstrated

Corrected.

Replies to E. Roussos' comments

1) Equation 1 is used to estimate radial gradients. However, N_1 & N_2 are count-rates, which are proportional to integral fluxes. Therefore, the estimated parameter is an "integral gradient". "Differential gradients" require to have differential flux measurements. For instance, it is my understanding that Gieseler & Heber (2016) estimate differential gradients, so comparison with the values obtained in this study should be reconsidered, even if values are similar.

Indeed, the data used in this study are counts that are proportional to integral fluxes. Differential GCR fluxes have not been yet extracted from the SREM data. Work is ongoing. In the manuscript, we now make it clear that our estimated parameter Gr is an integral gradient.

2) Both differential and integral gradients have an energy dependence. For the latter, which are more relevant to the present study, it matters above which energy fluxes are integrated. The used channel captures protons >49 MeV, however, from other SREM papers it seems that the geometry factor <100 MeV is rather low. So, I assume the estimated gradients have are for protons much above 100 MeV. Maybe folding the response function of the TS2 channel with a standard GCR spectrum can show which energies dominate.

The following plot show the SREM GCR response (the X-axis is the energy in MeV). We can see that TC2 is mostly sensitive to particles in the range [200-20000] MeV. We now indicate this range when we compare with previous results (see the updated section 3.2).

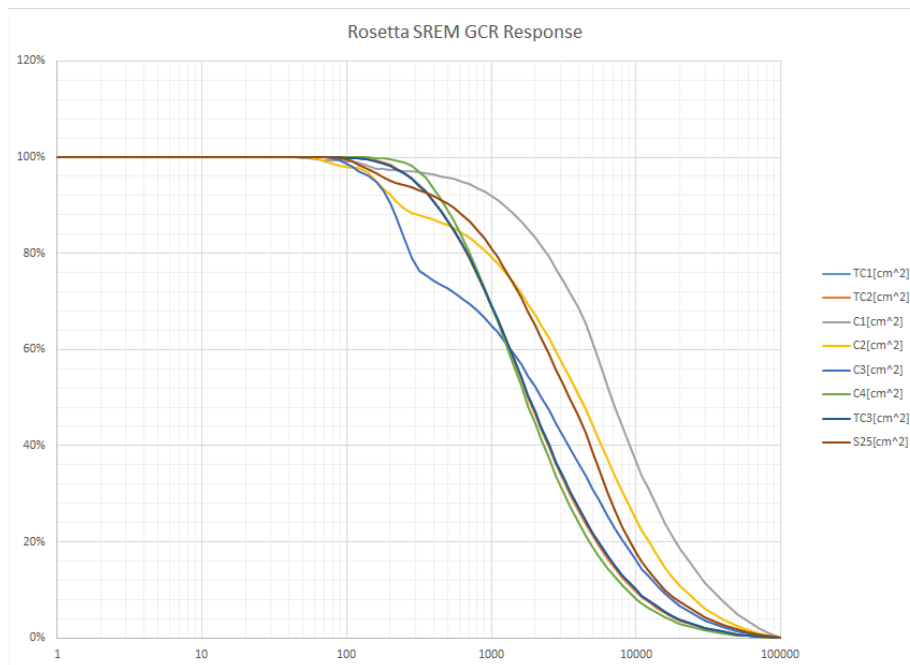


Figure 1: SREM GCR response

3) I am not sure how the HEND data are used in the study. In order for them to be compared with those from SREM, they have to be normalized to the INTEGRAL count rates, since SREM data are normalized to the INTEGRAL measurements. This means that in the y-axis of Fig. 3, one should use the INTEGRAL-normalized rates of SREM, not the raw SREM rates. I.e. this has to be a 2-step normalization. If that was actually done, it has to be clarified in the text.

This was actually done: we did a 2 step normalization: Rosetta to INTEGRAL and calibrated Rosetta to HEND. This is now clarified in the text.

4) After HEND data are normalized to SREM, they were not used in any part of the analysis. E.g. they may also be used to estimate radial gradients, which should be similar to those coming from the SREM/INTEGRAL ratios, otherwise they may be indicative of uncertainties in the gradient estimation, or, even better, of a radial dependence of the ratios. Instead, HEND are only mentioned briefly in lines 5-15 in p.11.

We found out (see the attached report, Thomas Honig's internship) that the HEND data set was not suitable for estimating the radial gradients. The data is too noisy. We used HEND in the analysis of the anticorrelation with interplanetary magnetic field and sunspot number (Annex 1). We have added more plots in this annex.

5) In addition to the comment above, it is clear that in the comet phase, where SREM sees a negative radial GCR gradient, the gradient between INTEGRAL/HEND is clearly positive, even if normalization may require an update (see comment 3). That further supports the possibility of a reduction of GCR fluxes around the comet. My suggestion is the following: a) Estimate the radial gradient between INTEGRAL/HEND for times during Rosetta's comet phase b) From this radial gradient, estimate what should have been the count rate of SREM c) Estimate the difference between the expected and the measured count-rate d) This difference may be estimated also by using in step (b) the average positive radial gradient as found from the data shown in Fig. 5 e) Then, the difference (estimated by any of the methods) could be organized as a function of heliocentric distance (essentially activity) or any other relevant parameter.

In fact, we applied this procedure (see attached report, internship report of Thomas Honig) with INTEGRAL. The steps were:

- a) Compute a radial gradient with the INTEGRAL and Rosetta data, for the time period covering the Rosetta cruise phase.*
- b) Assuming the same gradient for the comet phase, we simulated the Rosetta SREM count rate, from the INTEGRAL data, taking into account the correct distances.*
- c) When comparing the simulated and measured SREM count rates, we find this decrease in GCR count, see plot below.*

In order to make the article not too heavy, we did not explain this procedure, and we only included Figure 5 to illustrate the GCR “absorption”. Following this comment and the referee’s comments, we will now include a new figure (new figure 7):

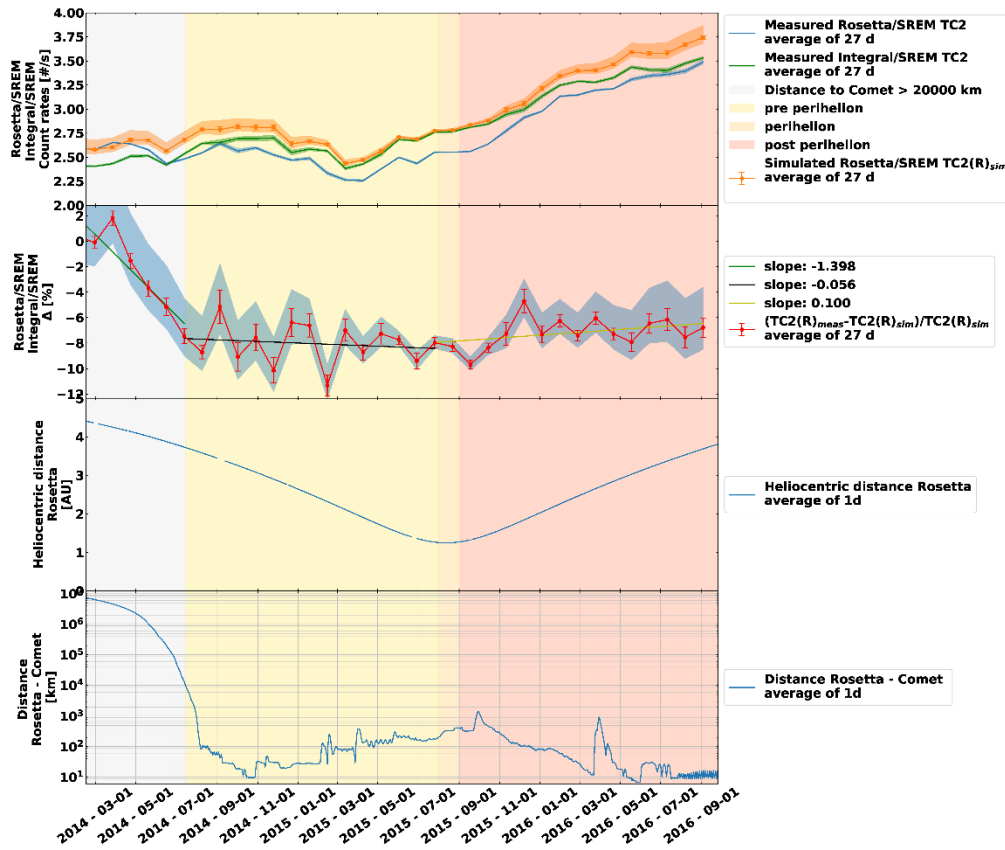


Figure 1: New Figure 7.

We have updated the text regarding the fact that the gradient between INTEGRAL/HEND is clearly positive (also following referee#2’s comment).

It appears intriguing that in Fig. 6, the count-rate difference appears to maximize around mid-2015, close to perihelion, and tends to become zero again towards the end of the mission.

We looked into more details about the behaviour of the GCR counts during the Rosetta comet science phase (see attached report and the new Figure 7 above), in particular to see the effect of heliocentric distance (comet activity), Rosetta-nucleus distances etc...However, we did not find anything relevant (so far).

I hope the authors find these comments helpful.

We thank Elias Roussos for these very helpful comments.

Replies to referee #1

We thank the referee for the careful review and all these very helpful comments. Our answers are in italic blue colour.

Typo: and spacecraft's component material->and a spacecraft's component materials

Corrected.

Figure 1b the lines are a little difficult to distinguish on the printed page and the dot dash and dashed lines are difficult to distinguish here.

Figure 1b has been updated as follows:

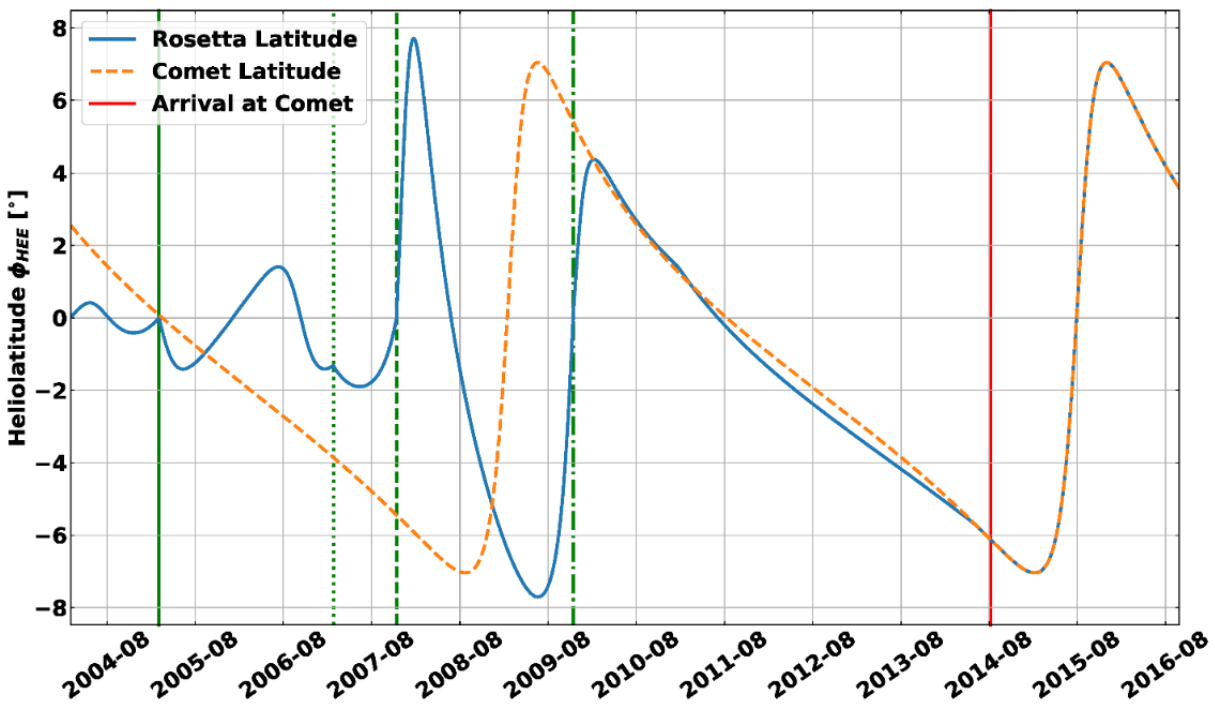


Figure 1: New Figure 1b

p5119 I would like more details on the process to remove SPEs. Anything above a local average is removed? Would a method such as a hampel filter be more appropriate here? I would like a little more detail here.

SPEs were removed in two steps.

Step 1):

Based on the „Solar Proton Event Archive“ (<http://space-env.esa.int/index.php/Solar-Proton-Event-Archive.html>) provided by NOAA SEC, SPEs were removed for all near Earth spacecraft. Following http://space-env.esa.int/index.php/NOAA_SPE_Template.html?date=19971104 :”The

Event selection criterion is when the NOAA/GOES-9 five minute averaged >10 . MeV $p+$ flux exceeds $2.0 p+/cm^2/s/sr$. The event is considered to have ended when the flux returns to below $1 p+/cm^2/s/sr$. Figure 2 shows an example of SPE period rejection. Since the data is based on geostationary satellites, further SPEs detected by HEND and Rosetta at locations with a significant longitudinal difference with respect to the Earth's heliocentric longitude had to be removed as discussed in step 2).

Step 2):

Numerical outlier detection was applied onto the data sets using a rolling mean outlier detection method. Due to the very noisy nature of the data set it turned out that one would either throw away too much data or would stick with still many outliers. Therefore it was decided to remove all non reported SPEs by hand.

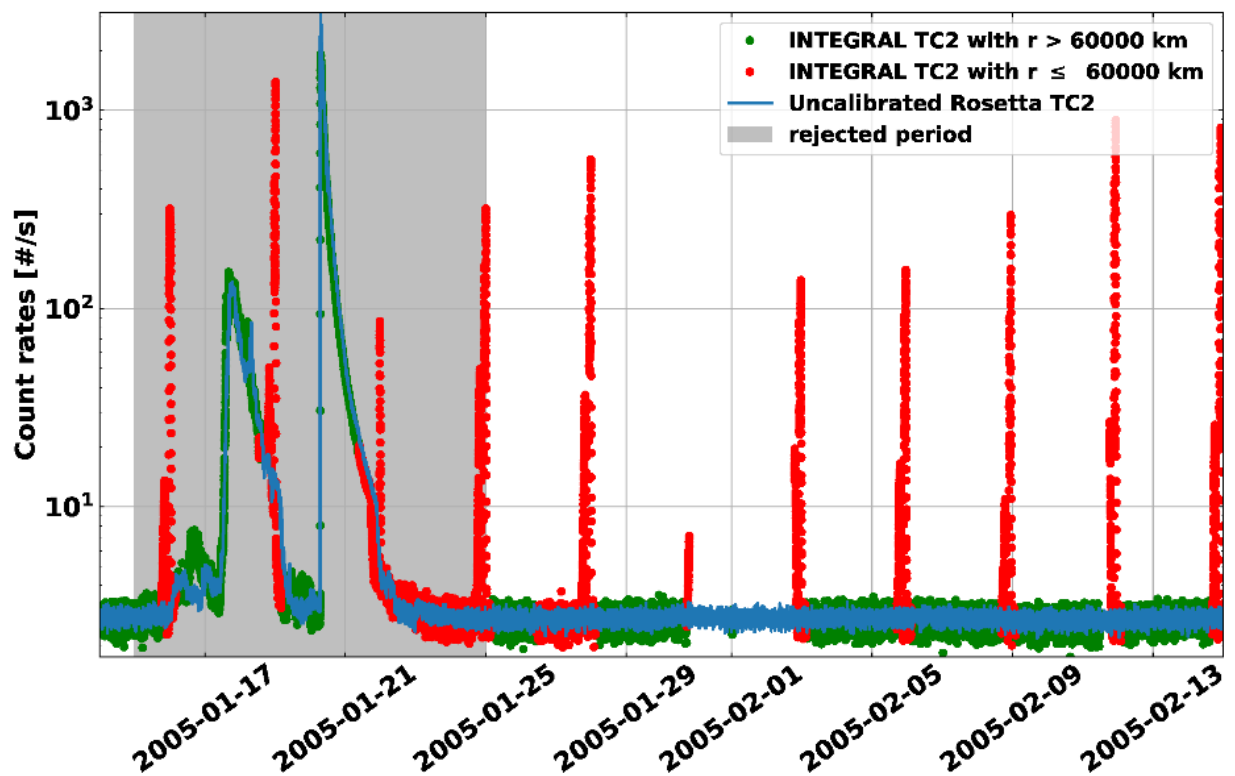


Figure 2: Example of SPE rejection for the INTEGRAL radiation monitor (for the referee only)

We have added the link to http://space-env.esa.int/index.php/NOAA_SPE_Template.html?date=19971104 in the relevant paragraph.

Figures 2 and 3 can you quote a value for the goodness of fit like χ^2

The χ^2 is now included. It is equal to ~ 4 in the case of Rosetta/INTEGRAL, and ~ 6 in the case of HEND/Rosetta.

Figure 4 and the related discussion the sun spot number is displayed but there is no source for this data. There are several different metrics which can be used as a 'sunspot number' see Lockwood 2014 and refs therein <https://doi.org/10.1002/2014JA019970>

Our source was : https://spitfire.estec.esa.int/ODI/dplot_ssn.html

This information was added in the acknowledgements.

Figure 4 what is the cadence of the data in Figure 4, are these averaged with over 27 days also?

Yes, we added labels to the plot stating this.

It would be interesting to also plot the variance or the standard deviation for the same window width as the averaging of the magnetic field as a proxy for the fluctuation amplitude of the magnetic field fluctuations.

Work is ongoing to see the effect of magnetic fluctuations (effect of turbulence), therefore we leave this activity for the near-future.

Replies to referee #2

We thank the referee for the careful review and all these very helpful comments. Our answers are in italic blue colour, while the updated text is in red.

GENERAL COMMENTS

SREM TC2 channel is a single detector channel. Since no coincidence/veto logics are applied, this channel could include a significant contribution from secondary particles induced by cosmic ray interaction with the s/c. Authors should at least briefly discuss if this is the case, as well as the relative importance of possible sources of background. Since the study covers a long time interval and a relatively wide range of radial distances, spatial and/or temporal variations of the background can be a critical issue for the analysis of quiet-time fluxes (GCR) and could affect the reliability of cross-calibrations along the period under analysis.

Indeed, secondary particles can influence the measurement. Considering different mass distributions of Rosetta and INTEGRAL, it can be assumed that this influence differs for each spacecraft. Under the assumption of a continuous impact averaged over the solar period of 27 days the rather, furthermore assumed, constant contribution might be different for Rosetta and INTEGRAL, but is expected to decrease significantly when performing the cross calibration in similar space environments.

A detailed study on the contribution by secondary particles could be a possible part in a follow-up study, although some work was already carried out at University of Oldenburg (Validation of flux models to characterize the radiation environment in space based on current Rosetta-data, Master thesis, 2017).

Section 2.4 now includes: The TC2 channel could include a significant contribution from secondary particles induced by cosmic ray interaction with the spacecraft itself. As a first approximation, this contribution is expected to be minimised in the cross-calibration process. A full characterisation could be the topic of a follow-up study.

SPECIFIC COMMENTS

Page 3, line 5. Although single detector channels such as TC2 are omnidirectional, it would be helpful for the later interpretation of the data to briefly describe the pointing of the Rosetta SREM aperture during the cruise phase and during the comet encounter.

We agree that it would be useful to study the pointing of the SREM detector, in particular for channels like C2 who are sensitive in a $\pm 20^\circ$ cone. This should be an interesting follow-up study. Since this study mainly concerns the TC2 channel, we did not spend too much time on it. We briefly discuss this point in Thomas Honig's internship report (see attached, section 5.10). In addition, for the referee, we show here how the comet 67P looks like in the SREM field of view.



Figure 1: SREM 20x20 field of view, 1 June 2016. Courtesy A. Sanderink.

P3 Table 1. The second column (logic) lists “D1” as logic for channels TC2 and S25. This seems inconsistent with e.g. page 2 line 26 and with Table 1 in Evans et al., 2008. Please check/correct since channel TC2 is the basis of the study presented in the manuscript. Instead of just providing a nominal “49 MeV to infinity” energy range, it would be valuable to discuss

the rigidity or energy range roughly represented by TC2 counting rates (taking into account the typical shape of the modulated GCR spectrum above 49 MeV and probably the energy-dependent instrument response). This information would be quite useful when comparing the inferred radial gradient with previously published results (Page 12).

Agreed; there was a mistake in Table 1. The table was updated and simplified. See below:

Table 1: new Table 1

Channel	Bin	Logic	Particles	Energy range (MeV)
1	TC1	D1	Protons	27-inf
			Electrons	2-inf
2	S12	D1	Protons	26-inf
			Electrons	2.08-inf
3	S13	D1	Protons	27-inf
			Electrons	2.23-inf
4	S14	D1	Protons	24-542
			Electrons	3.2-inf
5	S15	D1	Protons	23-434
			Electrons	8.08-inf
6	TC2	D2	Protons	49-inf
			Electrons	2.8-inf
7	S25	D2	Ions	48-270
8	C1	D1 x D2	Protons	43-86
9	C2	D1 x D2	Protons	52-278
10	C3	D1 x D2	Protons	76-450
11	C4	D1 x D2	Protons	164-inf
			Electrons	8.1-inf
12	TC3	D3	Protons	12-inf
			Electrons	0.8-inf
13	S32	D3	Protons	12-inf
			Electrons	0.75-inf

14	S33	D3	Protons Electrons	12-inf 1.05-inf
15	S34	D3	Protons Electrons	12-inf 2.08-inf

We agree that it would be more useful to provide more precise number than the “nominal “49 MeV to infinity” energy range”. However, this is clearly out of scope for this study. Nevertheless, for the TC2 channel, we can provide additional information. The following plot show the SREM GCR response (the X-axis is the energy in MeV). We can see that TC2 is mostly sensitive to particles in the range [200-20000] MeV. We now indicate this range when we compare with published results.

Added in table 1 caption: The study of the detector response to GCR indicates that the TC2 channels is mainly sensitive to energies between 200 MeV and 20 GeV.

New sentence in section 3.2: This result agrees well with previous studies for which the energy range can be compared with the TC2 range of ~0.2 – 20 GeV (e.g. Vos and Potgieter, 2016 / range 0.1-10 GeV; Gieseler and Heber, 2016 / range 0.45-2 GeV).

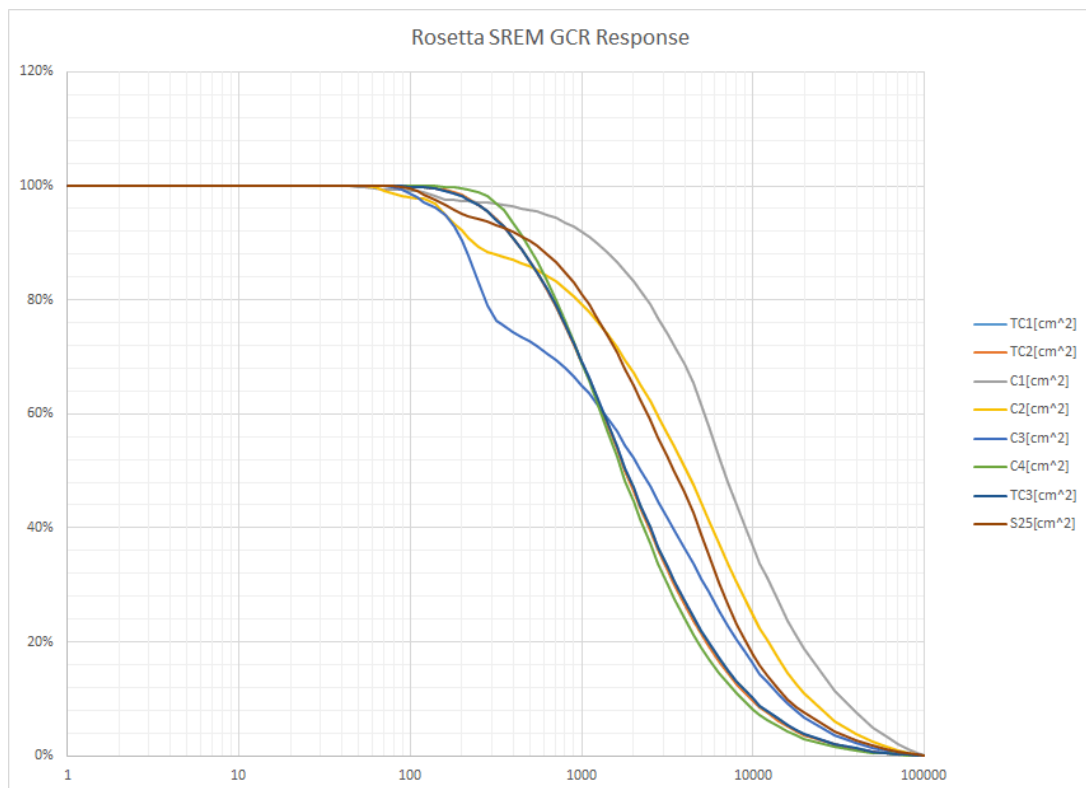


Figure 2: SREM detector response to GCR (for the referee only)

P4 Figure 1, bottom panel. Please define/clarify HEE, since this acronym normally stands for the Heliocentric Earth Ecliptic coordinate system and therefore latitudes would correspond to ecliptic latitudes and not to heliographic latitudes. Do the authors mean HEEQ (Heliocentric Earth Equatorial)? If not, replace “heliolatitude” by “ecliptic latitude”. This difference is also relevant for the discussion in P14L10.

“heliolatitude” was replaced by “ecliptic latitude”. Figure 1b was updated, see below.

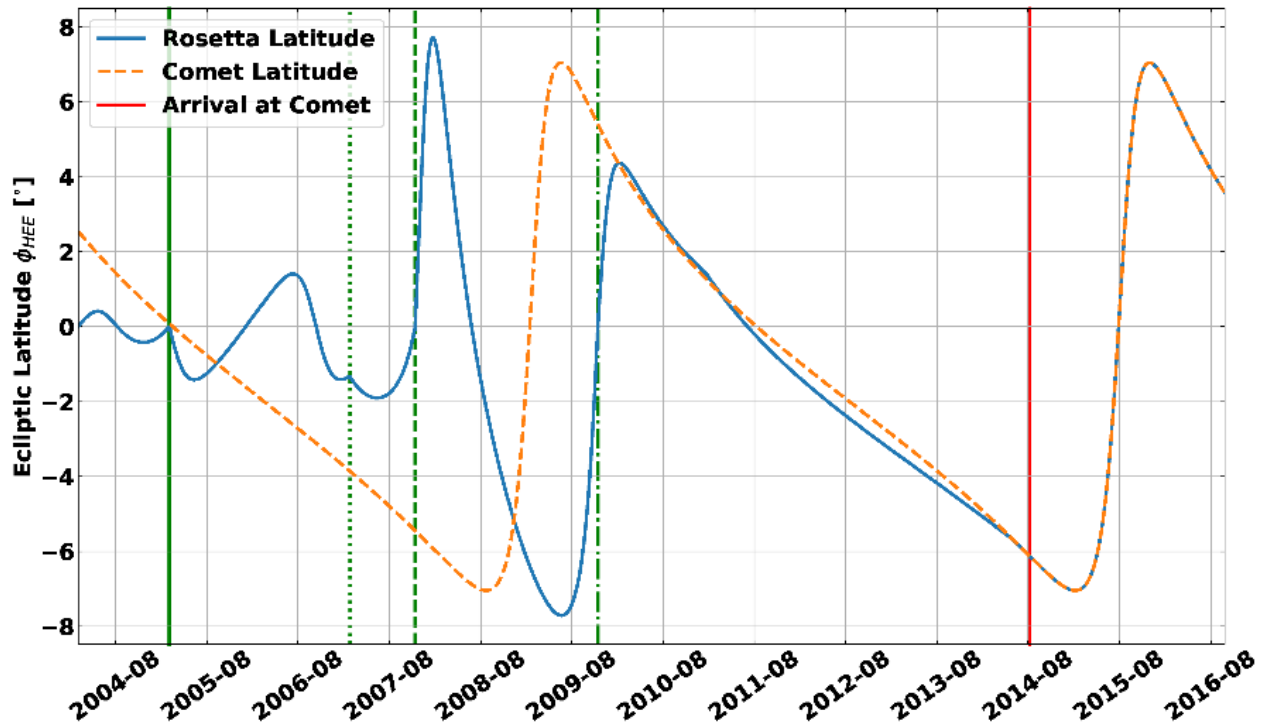


Figure 3: New Figure 1b

P5L19. The SREM channels and the exact procedure used to manually filter solar energetic particle events should be specified. Some events could be difficult to detect in TC2 (but still contribute) but become clearly visible at energies below 49 MeV.

SPEs were removed in two steps.

Step 1):

Based on the „Solar Proton Event Archive“ (<http://space-env.esa.int/index.php/Solar-Proton-Event-Archive.html>) provided by NOAA SEC, SPEs were removed for all near Earth spacecraft. Following http://space-env.esa.int/index.php/NOAA_SPE_Template.html?date=19971104 :”The Event selection criterion is when the NOAA/GOES-9 five minute averaged >10. MeV p+ flux

exceeds $2.0 \text{ p+}/\text{cm}^2/\text{s}/\text{sr}$. The event is considered to have ended when the flux returns to below $1 \text{ p+}/\text{cm}^2/\text{s}/\text{sr}$. Figure 2 shows an example of SPE period rejection. Since the data is based on geostationary satellites, further SPEs detected by HEND and Rosetta at locations with a significant longitudinal difference with respect to the Earth's heliocentric longitude had to be removed as discussed in step 2).

Step 2):

Numerical outlier detection was applied onto the data sets using a rolling mean outlier detection method. Due to the very noisy nature of the data set it turned out that one would either throw away too much data or would stick with still many outliers. Therefore it was decided to remove all non reported SPEs by hand.

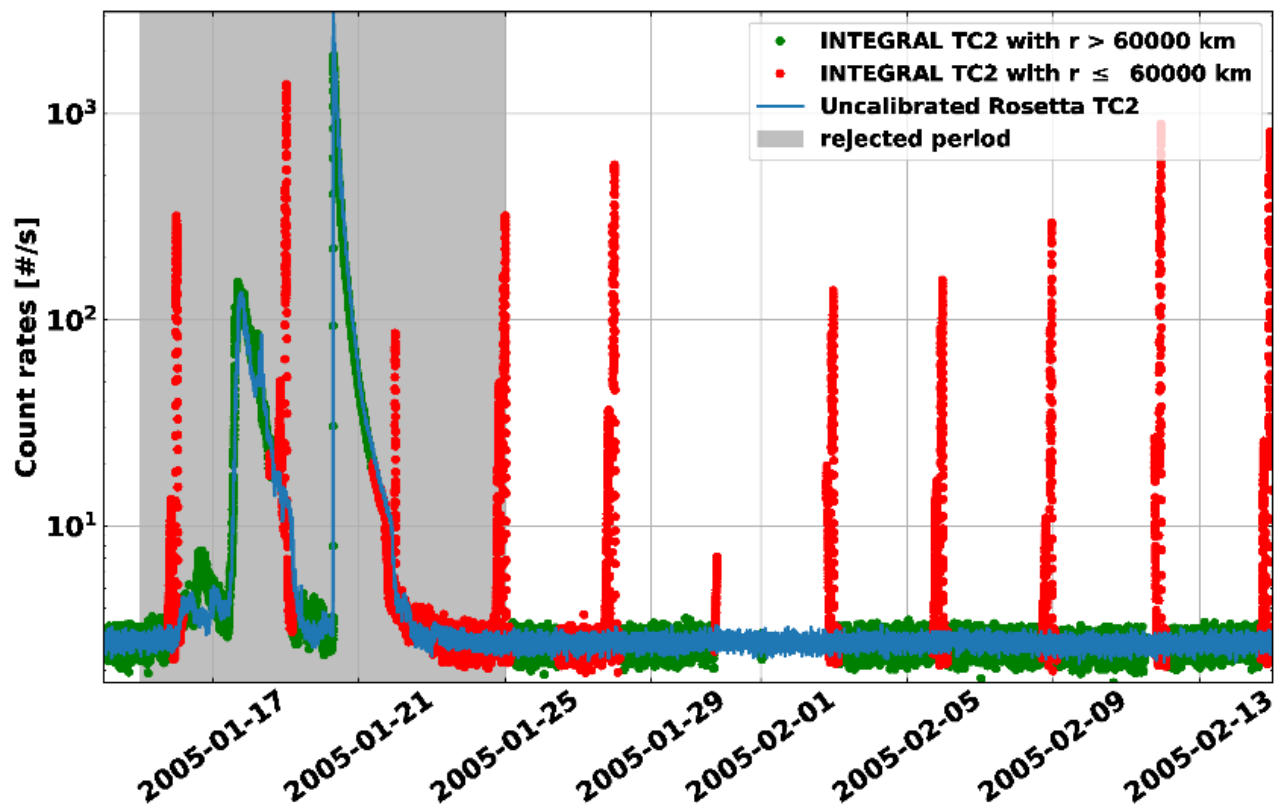


Figure 4: Removing SPE events (for the referee only)

The figure illustrates exemplarily how SPEs were removed by visual inspection (by removing the gray area) and how radiation belt influences on INTEGRAL were removed (red data points were removed with requirement: distance to Earth > 60000km). The quiet period as of 2005-01-25 also shows good agreement between uncalibrated Rosetta and INTEGRAL in a similar radiation environment on average.

We have added the link to http://space-env.esa.int/index.php/NOAA_SPE_Template.html?date=19971104 in the relevant paragraph.

P5L25. The reconfiguration of HEND should be explained with further detail. What is the ultimate reason for the count rate increase/offset?

In the HEND data set, there is the errata.txt file (http://pds-geosciences.wustl.edu/ody/ody-m-grs-2-edr-v1/odg1_xxxx/errata.txt) which report about this reconfiguration. This is the only public information that we found. The updated manuscript provides now this reference, in addition to [J. J. Plaut, personal communication]

P6L5-6. “We associate the 2.8% difference....with differences in the sensitivity area of the two SREM detectors”. Other factors such as noise levels, obstructions or different s/c mass distribution around the sensor head could contribute to this small difference between the nominally identical units onboard INTEGRAL and Rosetta (as well as Herschel, Planck and Proba-1).

Agreed; the updated manuscript now lists the other factors as well.

P7L23. Is this equation correct? The preceding text mentions that Proba-1 counting rates are systematically lower than INTEGRAL counting rates, then why is INTEGRAL rate (and not Proba-1 rate) multiplied by a number >1 in order to obtain a “corrected” Proba-1 rate directly comparable with INTEGRAL? The same question applies to the rest of cross-calibration equations. Probably this is just a notation problem, but it should be checked.

We have double checked and the cross calibration functions have to be changed as follows:

$$\begin{aligned} \text{Count}(\text{INTEGRAL}) &= 1.028 \times \text{Count}(\text{Rosetta}) - 0.127 / s \\ \text{Count}(\text{INTEGRAL}) &= 0.931 \times \text{Count}(\text{Herschel}) + 0.060 / s \\ \text{Count}(\text{INTEGRAL}) &= 0.938 \times \text{Count}(\text{Planck}) + 0.028 / s \\ \text{Count}(\text{INTEGRAL}) &= 1.256 \times \text{Count}(\text{Proba-1}) + 0.154 / s \\ \text{Count}(\text{Rosetta}) &= 0.035 \times \text{Count}(\text{HEND}) - 0.557 / s \end{aligned}$$

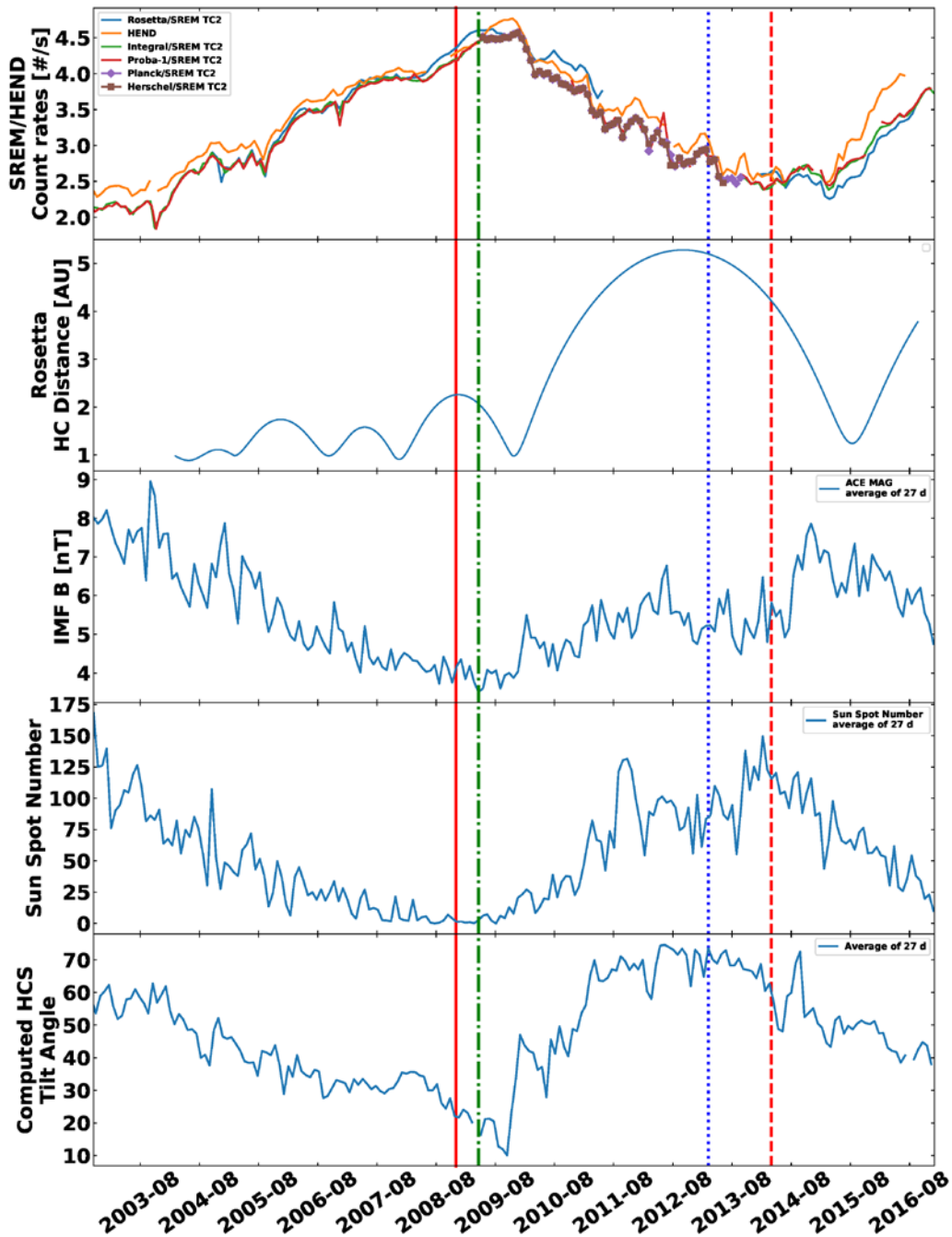
P8L6. See comment P7L23 above and clarify how the calibration factors are applied to HEND data in order to make them directly comparable with Rosetta.

We did a 2-step normalization: Rosetta to INTEGRAL and then calibrated Rosetta to HEND.

The text now says: The HEND neutron monitor HEND is calibrated with respect to SREM-Rosetta, which is calibrated with respect to INTEGRAL

P10 Figure 4. What is the reason for the peaks observed in HEND rates shortly after the vertical red dashed line? The difference between the near-Mars HEND and near- Earth SREM rates seem larger at the end of the plot (2015-16) than at the beginning (2003), while solar activity levels are comparable (although with opposite solar polarity). This, together with the comment on P5L25 raises some doubts about the stability of cross-calibration. Some discussion of these differences could be introduced e.g. in P11L7-8. Visibility of the different lines in the first panel could be improved.

Figure 4 was updated, see below:



The HEND spikes after the vertical red lines were removed, as part of the SPE removals. We should have done that for the submitted manuscript. The larger differences between HEND and INTEGRAL in 2015-2016 are not understood, and are now outlined in the manuscript.

P12L13-14. When citing agreement with Vos and Potgieter, 2016 and Gieseler and Heber, 2016, please mention the rigidity/energy ranges studied by these authors. The radial gradients presented here are based on counting rates accumulated over a broad energy

range, which makes difficult to define a reference energy for comparison (see comment about Table 1 above).

The text was updated accordingly: ... (e.g. Vos and Potgieter, 2016 / range 0.1-10 GeV; Gieseler and Heber, 2016 / range 0.45-2 GeV)

P12L16-17 and P14 Figure 6. “After that period, the count rate variation is in very good agreement with the expectation of a positive(?) radial gradient...”. This sentence sounds quite confusing since the Rosetta rates remain below the INTEGRAL rates till late 2016 (Figures 4 and 5 and discussion in following pages). In order to make easier the interpretation of Figure 6, I strongly suggest including panels showing the heliocentric distance of Rosetta and the distance between Rosetta and Comet 64P. In order to keep consistency with Figure 4, I also suggest plotting INTEGRAL SREM rates in green color.

There are three periods of interest:

- *Blue dots and red fit: Rosetta pre-hibernation data. Here we see the expected positive gradient, 2.96% per AU.*
- *Orange dots are January-July 2014: period when the attenuation of GCRs is noticed.*
- *Green dots and black fit: July 2014-September 2016. The attenuation is stable, and we see again the expected positive gradient, 2.9% per AU.*

The text now says: „After that period (green points and black fit), the count rate variation and the ratio is in very good agreement...“

Figure 6 was updated and made colors consistent. A new Figure was included (Figure 7) which displays the relevant distances. See below.

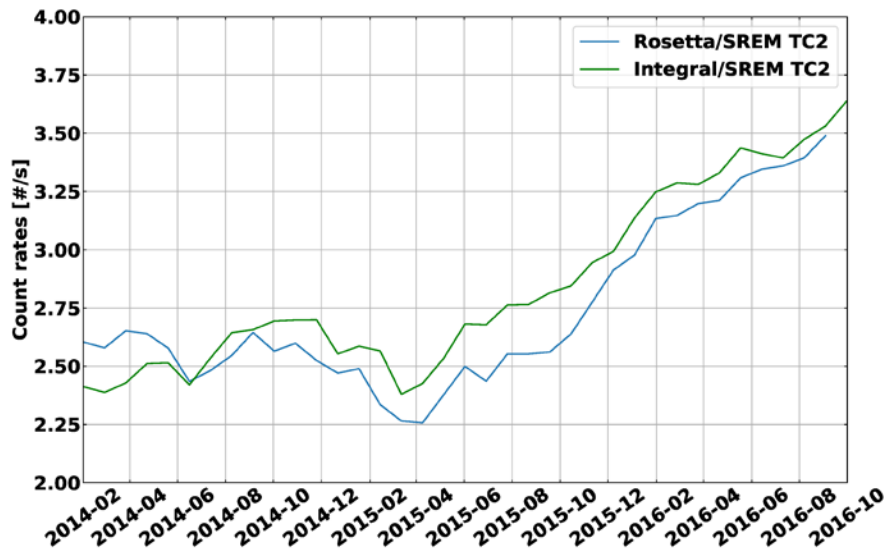


Figure 5: New Figure 6

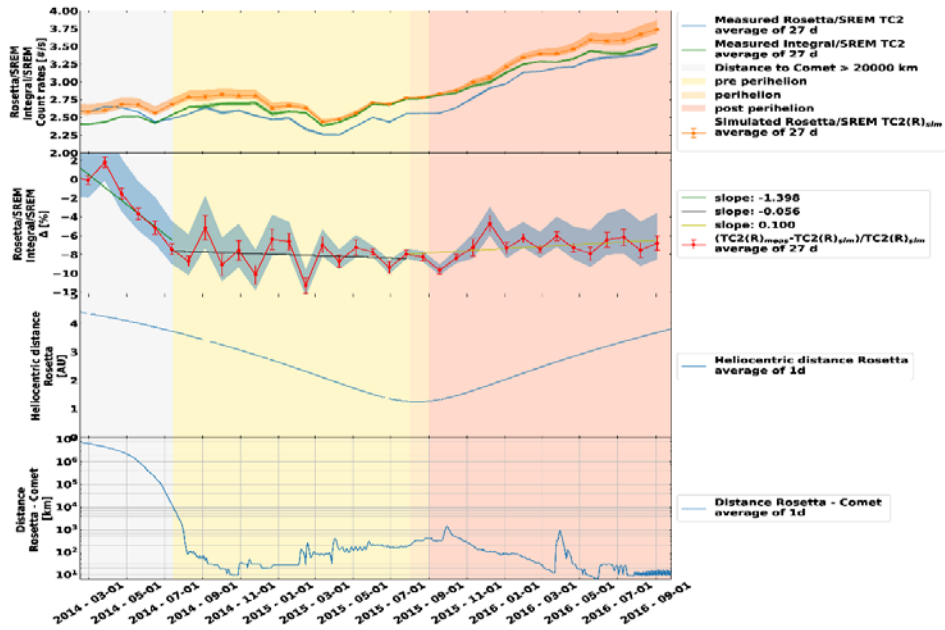


Figure 6: new Figure (figure 7), which includes the heliocentric distance of Rosetta and the Rosetta-comet distance.

P14L13. “The decreasing ratio begins when Rosetta reaches around 20,000 km from the cometary nucleus”. See comment above about including distance between Rosetta and the comet in Figure 6.

Figure 7 now includes the Rosetta-nucleus distance.

P14 and P15. Please briefly mention that the counting rates at Mars/HEND always stay higher than those registered near the Earth (Figure 4), even during the period shown in Figure 6. This is consistent with a permanent positive GCR radial gradient and supports that the reduction in the GCR rates at Rosetta compared to Earth is related to the comet approach.

The text was updated with the suggested sentences.

P15L16-17. In order to substantiate this suggestion, the authors should consider including and discussing the local plasma and magnetic field observations by Rosetta during the period shown in Figure 6.

Work is ongoing to see the effect of magnetic fluctuations (effect of turbulence); therefore, we leave this activity for the near future.

MINOR AND TYPOGRAPHIC COMMENTS

Affiliations: Please replace “Universitycity” by “University”.

Corrected.

Page 1, Line 21. “Major sources of this radiation are the Van Allen radiation belts, : : :”. The preceding sentences put the focus on missions outside the Earth’s magnetosphere, therefore this reference to radiation belts seems out of place.

Agreed. This reference was removed.

P2L4. “cover a range of heliocentric distances up to 3.5 AU”. Since Rosetta reached 4.5 AU, the term “heliocentric distance” sounds confusing here. Do the authors refer to the difference between the radial distances of two s/c, rather than to the Sun-s/c distance?

We understand the confusion. The word “heliocentric” was removed.

P2L9. “with two of them still operating: : :”. Please specify which ones.

Corrected.

P2L10. I suggest replacing “high energetic charged particles” by “high-energy charged particles” here and elsewhere in the manuscript.

Corrected in three places.

P3 Table 1. I suggest avoiding the redundant “MeV” labelling in the first and second line of the header, e.g. keeping it only in the first line.

Table 1 was updated and simplified, see above.

P3L21. “This sensor is the best one for space weather: : :”. Please reformulate this sentence in a more specific way.

“the best one” was changed by “very adequate”.

P4L11. Replace “Figure 1 shows: : :” by “Top panel of Figure 1 shows: : :”.

Corrected.

P5L5. Please, replace “and HEND’s orbits: : :” by “and Mars Odyssey’s orbits: : :”.

Corrected.

P5L15. What is the energy and/or intensity threshold of the Solar Proton Event list used here?

We refer here to an answer above.

P6L3. I suggest replacing “the fit curve” by “the linear fit”.

Corrected.

P7L20. Since the energy threshold of SREM TC2 is relatively low (49 MeV), magnetospheric shielding of the lower energy part of the GCR spectrum could also play a role here.

We used data above the magnetosphere (height above 60,000 km); therefore, we think that the magnetosphere has little effect.

P7L39. I suggest replacing “The neutron monitor HEND” by “The HEND neutron detector” or just “HEND- Mars Odyssey”.

Corrected.

P8L8. Indeed, the possible effect of Mars shadow would be implicitly included in the empirical cross-calibration procedure.

Since we did not do anything special, the Mars shadow is implicitly included in the cross-calibration.

P8 Table 2. Please add the units of b coefficient in the first row and include a and b uncertainties in the table.

The table was updated accordingly:

<i>Spacecraft 1</i>	<i>Spacecraft 2</i>	<i>a</i>	<i>Δa</i>	<i>b [1/s]</i>	<i>Δb [1/s]</i>
<i>INTEGRAL</i>	<i>Rosetta</i>	<i>1.028</i>	<i>0.005</i>	<i>-0.127</i>	<i>0.017</i>
<i>INTEGRAL</i>	<i>Herschel</i>	<i>0.931</i>	<i>0.001</i>	<i>0.060</i>	<i>0.005</i>
<i>INTEGRAL</i>	<i>Planck</i>	<i>0.938</i>	<i>0.001</i>	<i>0.028</i>	<i>0.005</i>
<i>INTEGRAL</i>	<i>PROBA-1</i>	<i>1.256</i>	<i>0.002</i>	<i>0.154</i>	<i>0.005</i>
<i>Rosetta</i>	<i>HEND</i>	<i>0.035</i>	<i>0.002</i>	<i>-0.557</i>	<i>0.025</i>

P10 Figure 4 caption, P11L10 and P11L27. Replace “sun spot” by “sunspot”.

Corrected.

P11L5 and P15L25 “solar rotation (27 days)” While this is OK for the purpose of smoothing longitudinal and transient variations at all locations, 27 days is just the Carrington (synodic and at intermediate latitude) solar rotation period. Therefore, I suggest removing “one solar rotation” and leaving just “27 days”.

Corrected.

P11L9 “different heliographic locations”. Do the authors mean “heliospheric locations”?

Corrected.

P11L12 “one of its orbits”.

Corrected.

P11L20 “long-term”.

Corrected.

P11L27 “anticorrelation: : :was calculated”. I suggest replacing either by “anticorrelation: : :was analyzed” or by “correlation coefficient: : :was calculated”.

Corrected.

P12L14 and P13L10 the term “comet phase” should be clarified/defined.

The comet phase refers to when Rosetta started its nominal mission around comet 67P. This is now clarified.

New text: “(the start of this phase is marked by the red vertical bar on Figure 1b)” was added after “The slope during the comet phase”.

P13L12. Replace “dark” by “black”.

Corrected.

P14L16 “hundreds of kg of propellant: : :etc.”. Could this mass loss significantly change the mass environment around the SREM detector and reduce the rate of secondaries contributing to TC2? For completeness, the authors could also mention the separation date of the Philae module and its (small) mass.

We checked during our study that the mass loss due to manoeuvres was not correlated with the SREM data variations.

We added the sentence “For completeness, we checked that the separation with the Philae module in November 2014 did not have noticeable effect.”

P15L22 “they are highly: : :”.

Corrected.

P15L29 “sunspot”.

Corrected.

P15L29. Please replace “annex” by “Annex 1”.

Corrected.

P15L30 Please replace “geographically” by “spatially”.

Corrected.

P15L31 “demonstrated”.

Corrected.

P16L3. The period corresponding to this radial gradient should be mentioned here.

“(between, 2004-10-21 to 2011-05-21)” was added.

P16L4 “this information provides”.

Corrected.

P18L27 Replace “cosmis” by “cosmic”.

Corrected.

P19L24 Replace “intergral” by “INTEGRAL”.

Corrected.

P22 Figure Annex 2. A panel showing the azimuthal separation between Rosetta and the Earth could be added to illustrate the origin of the time delays in the observed o-rotating structures.

Agreed;the azimuthal separation was added in the figure, see below. The caption was updated accordingly.

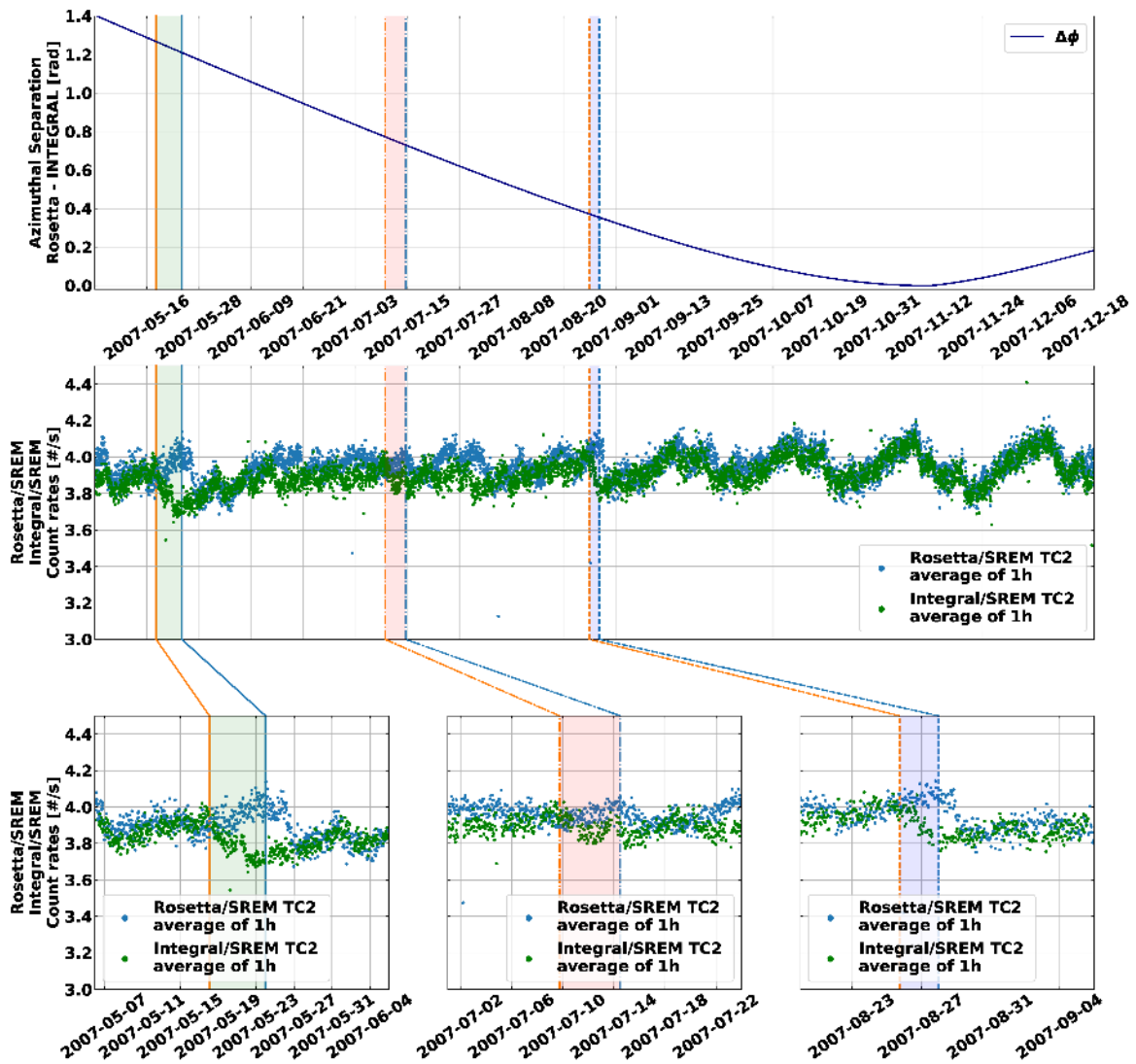


Figure 7: New Figure of Annex 2

The first panel shows the azimuthal separation between Rosetta and INTEGRAL. The second panel shows the count rates of channel TC2 as before. Both panels share the same x-axis (below first panel and above second panel). We see a nice (and expected) correlation between Rosetta and INTEGRAL approaching each other in terms of azimuthal separation and a decreasing time shift in the measured count rates until the point when delta phi vanishes and the count rates match well. Furthermore, color for INTEGRAL has been made consistent.

Multi-point galactic cosmic rays measurements between 1 and 4.5 AU over a full Solar cycle

Thomas Honig^{1,4}, Olivier G. Witasse¹, Hugh Evans¹, Petteri Nieminen¹, Erik Kuulkers¹, Matt G.G.T. Taylor¹, Bernd Heber², Jingnan Guo^{2,3}, Beatriz Sánchez-Cano^{4,3}

¹ European Space Agency, ESTEC, Noordwijk, 2200 AG, The Netherlands

² Institute of Experimental and Applied Physics, Christian-Albrechts-University, Kiel, Germany

³ School of Earth and Space Sciences, University of Science and Technology of China, Hefei, PR China

^{4,3} Department of Physics and Astronomy, University of Leicester, Leicester, United Kingdom

⁴ Johannes Gutenberg-University, Mainz, Germany

Correspondence to: Olivier Witasse (owitasse@cosmos.esa.int)

Abstract. The radiation data collected by the Standard Radiation Environment Monitor (SREM) aboard ESA missions INTEGRAL, ROSETTA, HERSCHEL, PLANCK and PROBA-1, and by the High Energy Neutron Detector (HEND) instrument aboard Mars Odyssey are analysed with an emphasis on characterising Galactic Cosmic Rays (GCRs) in the inner heliosphere. A cross-calibration between all sensors was performed for this study, which can also be used in subsequent works. We investigate the stability of the SREM detectors over long-term periods. The radiation data is compared qualitatively and quantitatively with the corresponding solar activity. Based on INTEGRAL and Rosetta SREM data, a GCR helioradial gradient of 2.96%/AU is found between 1 and 4.5 AU. In addition, the data during the last phase of the Rosetta mission around comet 67P/Churyumov-Gerasimenko were studied in more detail. An unexpected and yet unexplained 8% reduction of the Galactic Cosmic Ray flux measured by Rosetta SREM in the vicinity of the comet is noted.

1 Introduction

The space radiation environment affects both manned and unmanned missions outside the Earth's protecting atmosphere and its magnetic field. Highly energetic particles can penetrate living tissue and a spacecraft's component materials causing damage due to the deposition of energy. Major sources of this radiation are ~~the Van Allen radiation belts~~, Solar Energetic Particles (SEPs) and Galactic Cosmic Rays (GCRs). This work focusses on the third source, the GCRs, and in particular on their variations in the inner heliosphere. The variation in galactic cosmic rays intensity depends on different physical processes: inward diffusion in the interplanetary magnetic field, adiabatic cooling, outward convection and deceleration in the solar wind plasma, drift along the heliospheric current sheet, and interaction with magnetic structures in shocks and in interplanetary coronal mass ejections (e.g. McKibben; Potgieter, 2013; Morral 2013; Alania et al., 2014; Kozai et al. 2014; Giseler and Heber 2016). The GCR intensity is therefore varying with the solar wind velocity, the magnitude of the interplanetary magnetic field, solar activity, the heliospheric current sheet tilt angle, and the solar polarity change. ~~The variation of GCRs as a function of~~

different factors (solar cycle, heliocentric distance, solar wind conditions) is an interesting topic to explore, and lead to a better understanding of the heliosphere (e.g. Heber and Potgieter, 2008; Heber et al., 2013; Lawrence et al., 2016). The study of the effects of GCRs on the Earth's atmosphere and climate is also a fascinating field of research (e.g Carlaw et al., 2002; Pierce 2017, Everton et al., 2018).

5

This work is based on the analysis of data collected by the Standard Radiation Environment Monitor (SREM) units on Rosetta, Integral, Herschel, Planck and Proba-1 spacecraft and on data from the High Energy Neutron Detector (HEND) onboard Mars Odyssey. While Integral, Herschel, Planck and Proba-1 are located at around 1 AU from the Sun and HEND is orbiting Mars with an average heliocentric distance of 1.5 AU, Rosetta's heliocentric distance varied from 1 to 4.5 AU during its mission lifetime. This combined dataset provides a unique opportunity to determine the GCR flux measured over a range of heliocentric distances up to 3.5 AU and a time period of more than one solar cycle in interplanetary space. Of special interest are the Rosetta measurements close to comet 67P/Churyumov-Gerasimenko.

10

2 Instrument descriptions and data sets

2.1 The ESA radiation monitors

15

The SREM [e.g. Evans et al., 2008] is a particle detector developed to provide radiation information on a broad range of ESA space missions. SREM instruments have been installed on seven spacecraft so far, with two of them - PROBA-1 and INTEGRAL - still operating at the time of writing. With its ability to measure high-energy~~ye~~ charged particles (e.g. electrons and protons), it is able to provide valuable information regarding the near platform radiation environment, on short and long terms. In addition, measurements are also a valuable resource for the improvement of space radiation environment models.

20

The SREM instrument consists of two detector heads with three silicon diode detectors, denoted as D1, D2 and D3. In the first of the two detector heads, the detectors D1 and D2 are arranged in a telescope configuration with the main entrance covered by 2 mm of aluminium that provides a lower energy threshold of about 20 MeV for protons and about 1.5 MeV for electrons [Mohammadzadeh et al., 2003]. Additionally, the detectors are separated from each other by another 1.7 mm of aluminium and 0.7 mm of tantalum, which sets the threshold for protons up to roughly 39 MeV. Therefore, coincidence of D1 and D2 measures mostly high-energy~~ye~~ protons. The opening window for the remaining detector head corresponding to detector D3 is covered with 0.7 mm of aluminium and provides therefore an energy threshold of about 0.5 MeV for electrons and about 10 MeV for protons, respectively. The opening angle of the telescope is ± 20 degrees. The detector electronics can operate with a detection rate up to 100 kHz with a corresponding dead-time correction below 20%. The instrument itself is a box of 20x12x10 cm³ which weighs 2.6 kg including the detector system and the supporting electronics. Measuring the incident radiation, the particle events are binned into 15 different channels which have different energy thresholds and discriminator levels. This allows a differentiated insight into the energy ranges of the events. Table 1 displays the channels with corresponding logic.

25

30

particles species, and energy thresholds range and discriminator levels. Channels TC1, S12, S13 (all D1) and TC2 (D2) are sensitive to both electrons and protons, where TC2 has the highest energy threshold of about 49 MeV for protons and about 2.8 MeV for electrons. With the channels S14, S15, C1-C3, S33 and S34 it is possible to measure mainly protons due to the given energy thresholds and the comparatively high discriminator levels. Channel S25 is dedicated to measure the generally very low heavy ion flux due to its very high discriminator level. However, previous studies point to the fact that the heavy ion channel is most sensitive to protons [Ludecke et al., 2017]. The coincidence channels C1 to C4 use both detector D1 and D2 simultaneously and measure mainly protons due to the high shielding provided by the layers made of aluminium and tantalum. The insensitivity of the C1, C2 and C3 channels to electrons arises from the high energy deposit thresholds for these channels. The threshold for C4 is low enough to detect the electrons that can make it through the shielding. Channels TC3 and S32 to S34, based on detector D3, are sensitive to low energy protons with the sensitivity to electrons diminishing from S32 to S34. Nevertheless, one should keep in mind that all channels measure electrons as well as protons and that all channels are correlated. This means that it is possible to measure the same event in multiple channels. While the single detector channels tend to measure particles in an omnidirectional way, the coincidence channels can be characterized to measure particles with a certain directionality. Therefore, there is a reduced number of degrees of freedom since the particles are required to deposit energy in D1 and D2 simultaneously, and this is only possible if the particle trajectory crosses both detectors.

Bin	Logic	Discriminator Level $\Delta E > XX$ [MeV]	Proton Energy [MeV]			Electron Energy [MeV]		
			Min [MeV]	Max [MeV]	SCF [# / cm ²]	Min [MeV]	Max [MeV]	SCF [# / cm ²]
TC1	D1	0.085	27	∞	15.8	2.0	∞	118
S12	D1	0.25	26	∞	19.0	2.08	∞	195
S13	D1	0.6	27	∞	16.0	2.23	∞	519
S14	D1	2.0	24	542	38.5	3.2	∞	25403
S15	D1	3.0	23	434	65.6	8.18	∞	5460
TC2	D1	0.085	49	∞	13.1	2.8	∞	191
S25	D1	9.0	48	270	208.8	n/a	n/a	
C1	D1×D2	0.6, 2.0	43	86	107.22	n/a	n/a	
C2	D1×D2	0.6, 1.1 - 2.0	52	278	75.6	n/a	n/a	
C3	D1×D2	0.6, 0.6 - 1.1	76	450	35.1	n/a	n/a	
C4	D1×D2	0.085 - 0.6, 0.085 - 0.6	164	∞	10.4	8.1	∞	155
TC3	D3	0.085	12	∞	49.3	0.8	∞	101
S32	D3	0.25	12	∞	49.3	0.75	∞	189
S33	D3	0.75	12	∞	40.2	1.05	∞	1162
S34	D3	2.0	12	∞	63.8	2.08	∞	93077

Channel	Bin	Logic	Particles	Energy range (MeV)
1	TC1	D1	Protons Electrons	27-inf 2-inf

Formatted Table

2	S12	D1	Protons Electrons	26-inf 2.08-inf
3	S13	D1	Protons Electrons	27-inf 2.23-inf
4	S14	D1	Protons Electrons	24-542 3.2-inf
5	S15	D1	Protons Electrons	23-434 8.08-inf
6	TC2	D2	Protons Electrons	49-inf 2.8-inf
7	S25	D2	Ions	48-270
8	C1	D1 x D2	Protons	43-86
9	C2	D1 x D2	Protons	52-278
10	C3	D1 x D2	Protons	76-450
11	C4	D1 x D2	Protons Electrons	164-inf 8.1-inf
12	TC3	D3	Protons Electrons	12-inf 0.8-inf
13	S32	D3	Protons Electrons	12-inf 0.75-inf
14	S33	D3	Protons Electrons	12-inf 1.05-inf
15	S34	D3	Protons Electrons	12-inf 2.08-inf

Formatted: Normal

Formatted: Normal

Formatted: Normal

Formatted: Normal

Formatted: Normal

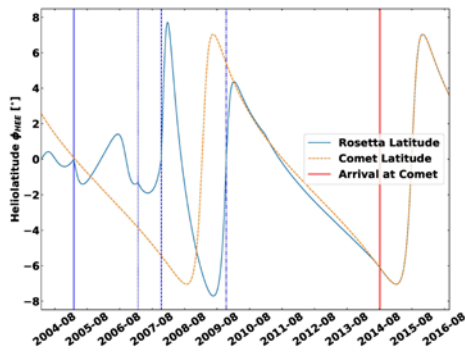
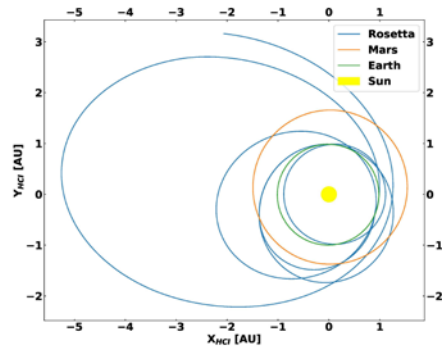
Formatted: Normal

5 Table 1: List of SREM energy channels. The column 'BIN' gives the name of the channel, and the column 'Logic' names the corresponding detector, the column 'Discriminator Level' defines the minimum energy to be deposited, the columns 'Proton Energy' and 'Electron Energy' define the given energy threshold of the channel and the Single Conversion Factor (SCF) to derive differential fluxes from count rates (from adapted from Evans et al., 2008). The study of the detector response to GCR indicates that the TC2 channels is mainly sensitive to energies between 200 MeV and 20 GeV.

2.2 HEND

In addition to the SREM monitors, we have used data recorded by the High Energy Neutron Detector (HEND) [Boynton et al., 2004] on board the Mars Odyssey spacecraft. It is composed of five separate sensors that provide measurements of neutrons
5 in the energy range from 0.4 MeV up to 15 MeV. In this study, only data from the Outer Scintillator (a veto-counter and used
for anti-coincidence rejection of charged particles) in channels 9–16 is used (~195->1000 keV). This sensor is the best one every
adequate for space weather studies as it is sensitive to neutrons, charged particles, and energetic photons (see more information
at Sanchez-Cano et al., 2018). This instrument can be used also as a proxy for GCRs, as demonstrated in Zeitlin et al. (2010),
since HEND measure secondary particles produced by the interactions of primary energetic GCR with the spacecraft, providing
10 indirectly a measure of the cosmic rays (Zeitlin et al. 2010).

2.3 Orbits



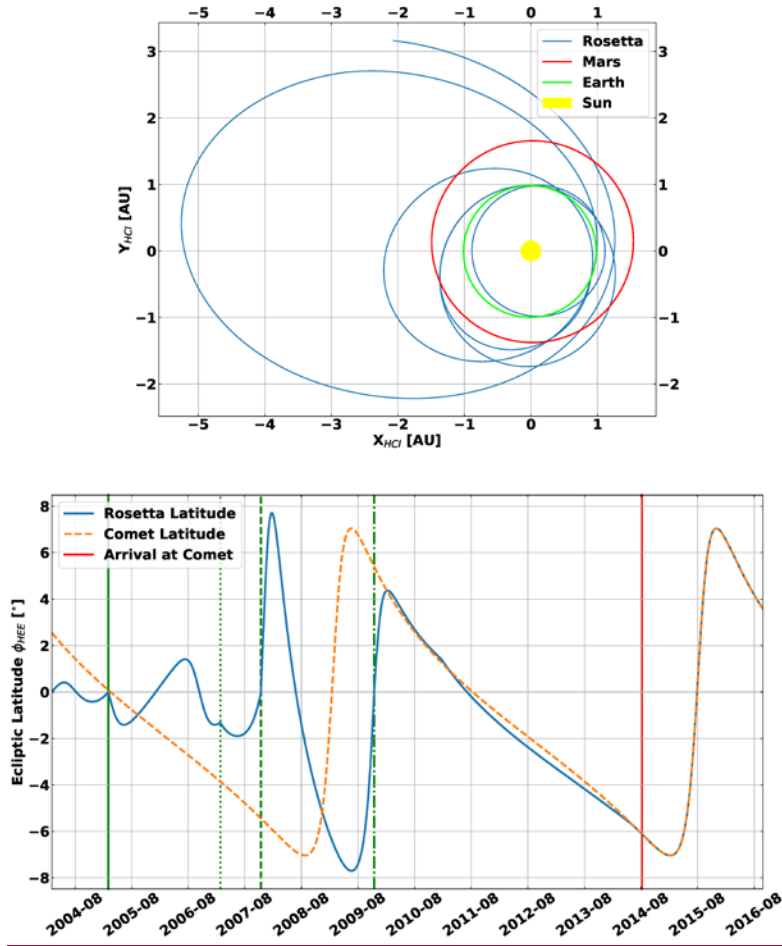


Figure 1: Orbital information for the used data sets. Top panel: Orbits of Earth (green), Mars (red/orange) and Rosetta (blue) in HCI coordinates. Bottom panel: Helio Ecliptic latitude in HEE coordinate system, the solid green/blue line indicates the first Rosetta Earth flyby, the dotted green/blue line indicates the Mars flyby, the dashed green/blue line indicates the second Earth flyby and the dashed dotted green/blue line indicates the third Earth flyby.

5

Top panel of Figure 1 shows the orbits of Earth (green), Mars (orange) and Rosetta (blue) in Helio-Centric Inertial (HCI) coordinates. The HCI coordinate system is defined with its x-axis pointing towards the Solar-ascending node on the ecliptic, the z-axis to be aligned with the solar rotational axis and the y-axis completing a right-handed Cartesian triad. At scales of AU, we can assume that Earth's orbit is similar to INTEGRAL, Proba-1, Herschel and Planck's orbits and that the Mars' and HEND's Mars Odyssey's orbits have also a similar orbit around the Sun. The second panel of Figure 1 illustrates the heliolatitudes travelled by the Rosetta mission, which describes how far the spacecraft and the comet travel out of the ecliptic plane. While the comet's components reflect its periodic nature, Rosetta's components do not, since it underwent a number of orbital changes to attain the same orbit as the comet. This was achieved with several gravity assist flybys, which are indicated on the plot by vertical lines: three Earth gravity assists on 2005-03-04 (solid), 2007-11-13 (dashed) and 2009-11-13 (dashed dotted) and a Mars gravity assist on 2007-02-25 (dotted) which all had a significant impact on the trajectory of the spacecraft. The final vertical line, in red, indicates the comet rendezvous on 2014-08-06.

2.4 Data processing

In this section, we explain the procedure of the GCR analysis. SREM channel TC2 was chosen to be the main channel for this study, having the highest proton energy threshold of the non-coincidence counters with about 49 MeV. Since the GCR spectrum is dominated by very high-energy α particles, it is therefore the most sensitive channel for these purposes.

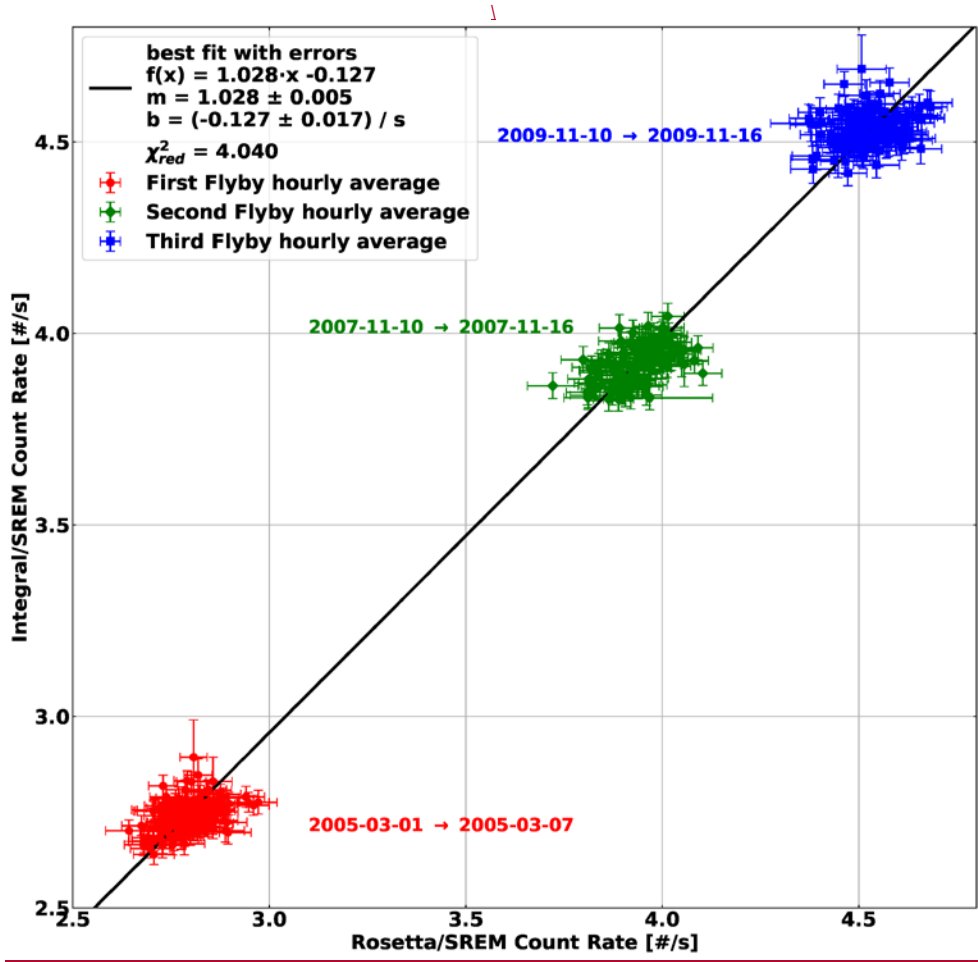
The TC2 channel could include a significant contribution from secondary particles induced by cosmic ray interaction with the spacecraft itself. As a first approximation, this contribution is expected to be minimised in the cross-calibration process. A full characterisation could be the topic of a follow-up study. As this study focuses on a count rate spectrum consisting of GCRs, it is necessary to clean the data sets from solar proton events (SPE) contamination, by removing intervals containing SPE events.

The times were chosen based on the ESA Solar Proton Event Archive' (<http://space-env.esa.int/index.php/Solar-Proton-Event-Archive.html>). Since the data in this archive are based on geostationary satellites, further SPEs detected by HEND and Rosetta at locations with a significant longitudinal difference with respect to the Earth's heliocentric longitude had to be removed manually. In practice, we removed peaks associated with SPEs in data when SPEs exceeded a local daily mean value of count rates (see http://space-env.esa.int/index.php/NOAA_SPE_Template.html?date=19971104 for more details). The INTEGRAL data set needed an additional processing to remove the signatures of Earth's inner magnetosphere trapped particle environment, by only considering spacecraft altitudes above 60,000 km from the origin of the geocentric equatorial inertial (GEI) coordinate system.

The HEND data had to be processed in multiple steps. First, the SPEs were removed in a similar procedure as for the SREM data. Second, the reconfiguration of the anti-coincidence switch on HEND in 2012 had to be taken into account. This correction manifests itself in a constant offset of 750 counts from 2012-10-19 16:02:54 [J. J. Plaut, personal communication, and see http://pds-geosciences.wustl.edu/ody/ody-m-grs-2-edr-v1/odg1_xxxx/errata.txt] which can be easily reversed. Finally, the data were converted from count to counts per second by considering a collection interval of 19.7 seconds [Zeitlin et al., 2010].

2.5 Cross-calibration between radiation monitors

A quantitative comparison between the measured count rates from different radiation monitors on spacecraft requires a cross-calibration exercise. All SREM instruments were calibrated against the INTEGRAL sensor, as INTEGRAL offers the longest baseline. HEND was then calibrated to the calibrated SREM on-board Rosetta. The calibration of Rosetta to INTEGRAL was based on their hourly averaged data of three days around Rosetta's three Earth flybys (similar space radiation environment during the flybys) on 2005-03-04, on 2007-11-13 and on 2009-11-13. A linear fit of the data sets is performed from which a fit function can be obtained. The latter is used to calibrate the Rosetta/SREM channel TC2 data. Figure 2 displays the three hourly averaged data sets with the corresponding standard error, together with the linear fit curve. The data appear well aligned during the three chosen calibration periods, suggesting similar response to the GCR radiation environment and good stability over time between Rosetta and INTEGRAL. We associate the 2.8% difference between INTEGRAL and Rosetta, taken from the gradient fit of 1.028 ± 0.005 , with differences in the sensitivity area of the two SREM detectors, noise levels, obstructions or different spacecraft mass distribution around the sensor head. We associate the GCR count rate changes over the years to be associated with the solar cycle (e.g. Heber and Potgieter, 2008; Potgieter, 2013) which is discussed in more depth below.



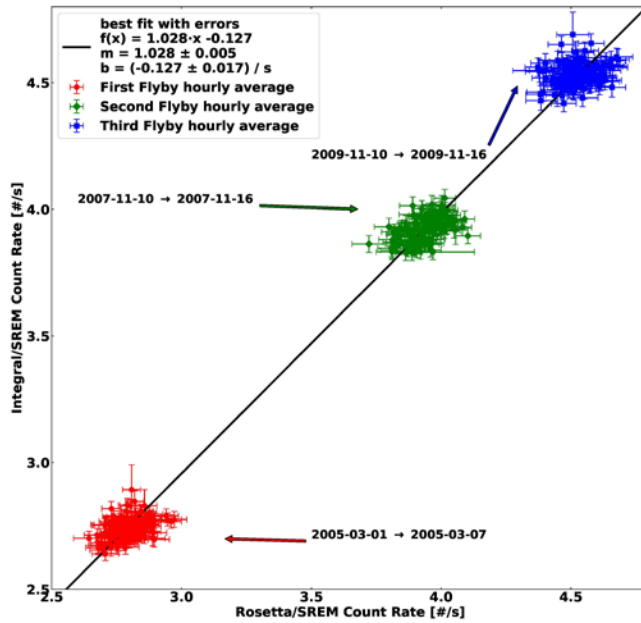


Figure 2: Cross-calibration between INTEGRAL and Rosetta SREM instruments. Fitted data of Rosetta SREM and INTEGRAL SREM channel TC2 for the time around Rosetta's Earth flybys.

5

The fit yields the calibration function of equation:

$$10 \text{ Count (INTEGRAL}_{\text{Rosetta}}) = 1.028 \times \text{count (ROSETTA}_{\text{INTEGRAL}}) - 0.127 / s$$

This function is then applied on the whole data set of channel TC2.

Calibration of Planck/SREM, Herschel/SREM and Proba-1/SREM to INTEGRAL/SREM

15

Under the assumption that Planck, Herschel and INTEGRAL measure in a similar space radiation environment, excluding the INTEGRAL radiation belt passages, the calibration of Planck and Herschel to INTEGRAL is based on the whole channel TC2 data set of the spacecraft at Lagrange point L2 to ensure the highest statistics and therefore most accurate fit possible. The fit yields the following calibration functions:

5
Count (~~INTEGRAL~~Herschel) = 0.931 x count (Herschel/~~INTEGRAL~~) + 0.060 / s
Count (~~INTEGRAL~~Planck) = 0.938 x count (Planck/~~INTEGRAL~~) + 0.028 / s

10 Cross- calibration with Proba-1 was carried out in a similar way to Planck and Herschel, although in this case, INTEGRAL counts were consistently higher than Proba-1 by a factor of 1.256. In addition to a possible active area difference, PROBA-1's lower count rates can easily be explained by its low altitude orbit, with the solid angle of Earth presenting a shielding for GCR fluxes. The fraction of the solid angle divided by 4 pi is equal to 21.2 %.

The fit yields the calibration function:

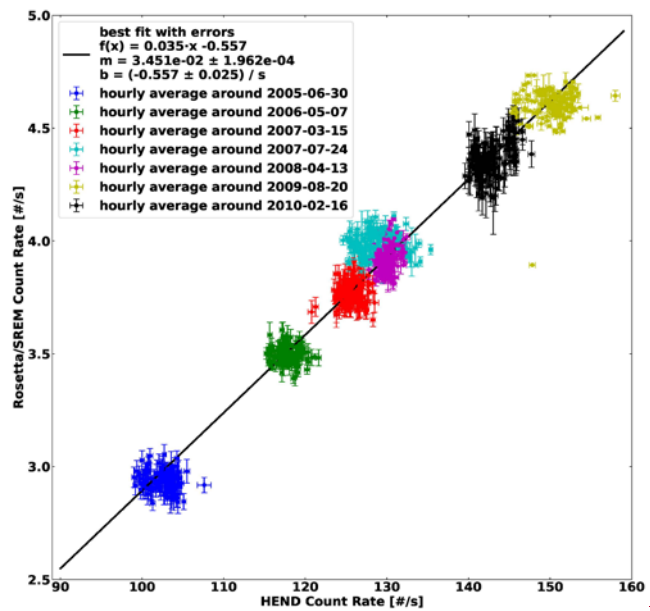
15 Count (~~INTEGRAL~~Proba-1) = 1.256 x count (~~INTEGRAL~~PROBA-1) + 0.154 / s

This function is applied on the whole data set of Proba-1's channel TC2.

HEND

20 The HEND neutron monitor ~~HEND~~ is calibrated with respect to SREM-Rosetta, which is calibrated with respect to INTEGRAL. Assuming a mean heliocentric distance of Mars at 1.5 AU, Rosetta data were used when the spacecraft was located at the same distance from the Sun, which happened seven times during the Rosetta cruise. These periods are indicated in Figure 3, each covering +/- 3 days around the indicated time and made up of hourly averaged data.

25



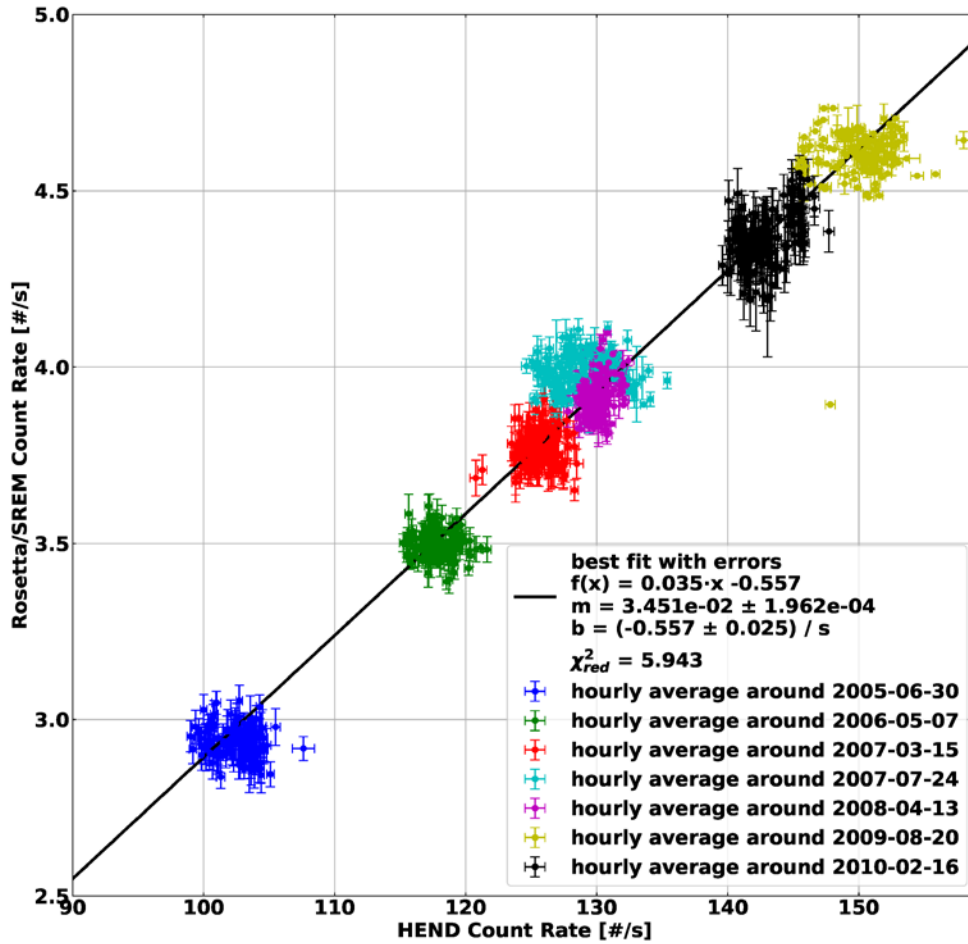


Figure 3: Cross-calibration of Mars Odyssey HEND with Rosetta SREM, calibrated against INTEGRAL data. The seven groups of data correspond to the seven times Rosetta was at 1.5 AU from the Sun.

The fit yields the calibration function:

5

$$\text{Count (RosettaHEND)} = 0.035 \times \text{count (RosettaHEND)} - 0.557 / s$$

This function is applied to the whole HEND data set. It should be also noted that the shadow of Mars is not included in this study. The corresponding shielding is expected to be about 20 %.

5 Table 2 lists the fitting parameters, for the generic function: count (spacecraft 1) = a x count (spacecraft 2) + b

Spacecraft 1	Spacecraft 2	a	Δa	b [1/s]	Δb [1/s]
INTEGRAL	Rosetta	1.028	0.005	-0.127	0.017
INTEGRAL	Herschel	0.931	0.001	0.060	0.005
INTEGRAL	Planck	0.938	0.001	0.028	0.005
INTEGRAL	PROBA-1	1.256	0.002	0.154	0.005
Rosetta	HEND	0.035	0.002	-0.557	0.025

- Formatted: Font: Not Italic
- Formatted: Font: Not Italic
- Formatted: Font: Not Italic
- Formatted: Font: Not Italic
- Formatted: Font: Not Italic
- Formatted: Font: Not Italic
- Formatted: Font: Not Italic
- Formatted: Font: Not Italic

Spacecraft 1	Spacecraft 2	a	b
Rosetta	INTEGRAL	1.028	-0.127
Herschel	INTEGRAL	0.931	0.060
Planck	INTEGRAL	0.938	0.028
Proba-1	INTEGRAL	1.256	0.154
Mars-Odyssey	Rosetta	0.035	-0.557

10 Table 2: Fitting parameters for the function: count (spacecraft 1) = a x count (spacecraft 2) + b, including their uncertainties.

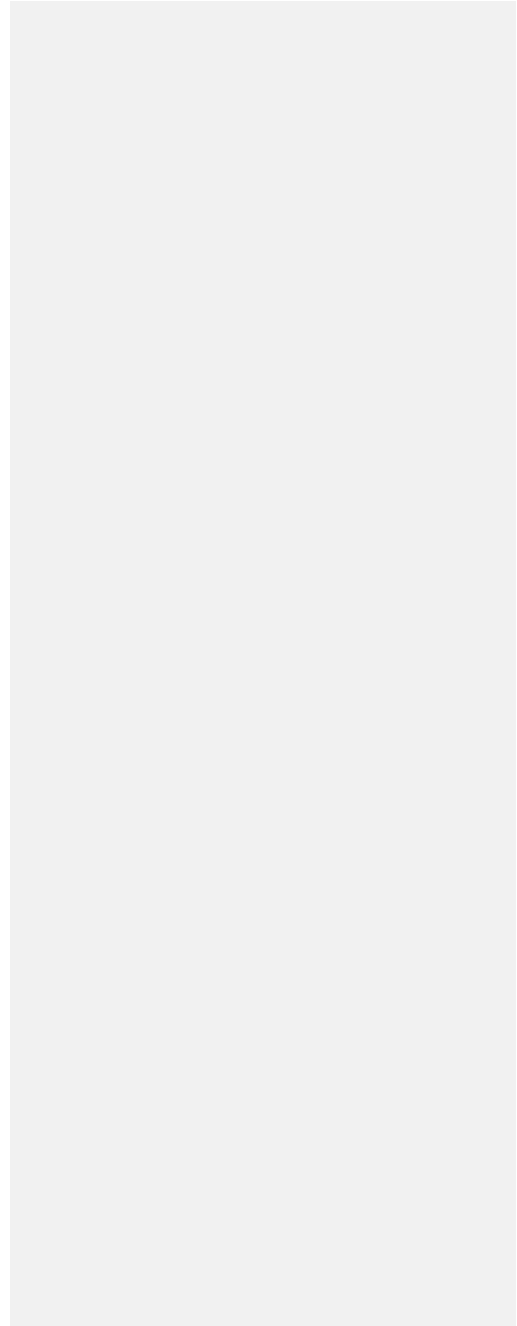
15

20

5

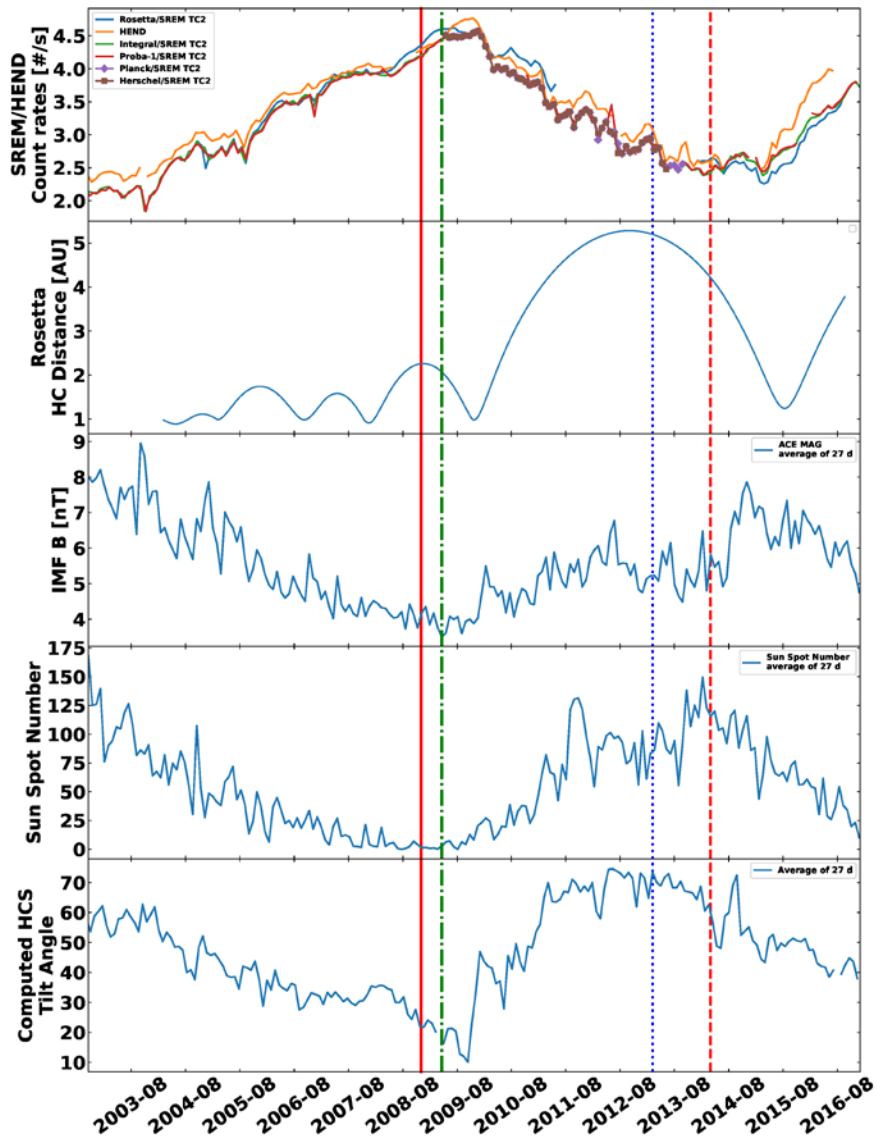
10

15



3 Data analysis

3.1 Overview of the data, GCR modulation



Formatted: Normal, Centered

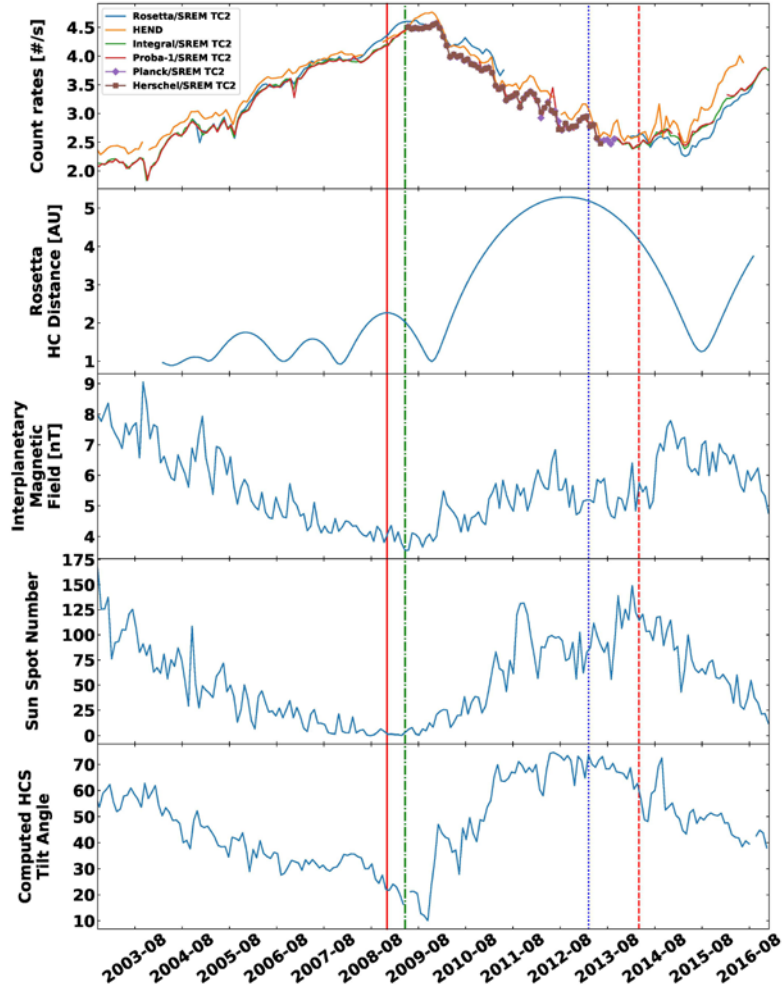


Figure 4: Temporal evolution of various data sets. 1st panel: SREMs and HEND count rates averaged over 27 days. 2nd panel: Rosetta Heliocentric distances. 3rd panel: Interplanetary magnetic field measured by ACE at 1AU. 4th panel: Sun-spot number. 5th panel: Computed tilt angle of the heliospheric current sheet. The solid red vertical line indicates the minimum sunspot number while the dashed vertical line indicates the maximum sunspot number. The dash-dot green vertical line indicates the peak of the Rosetta SREM count rate. The dotted blue line indicates the reversal of polarity of the average solar polar flux.

Having implemented the appropriate cross-calibrations, a qualitative and quantitative comparison of the obtained data sets is possible. Data are averaged over ~~one solar rotation~~ (27 days) in order to minimize longitudinal effects. Such longitudinal effects are illustrated in Annex 2. In the upper panel of Figure 4, radiation data of Rosetta/SREM, INTEGRAL/SREM, Planck/SREM, Herschel/SREM, Proba-1/SREM and HEND are shown. The SREM and HEND data are very well aligned throughout the whole epoch, although some differences do stand out, in particular for HEND and Rosetta, which we associate with different heliospheric locations. The larger differences between HEND and INTEGRAL in 2015-2016 are not understood. The other panels display the Rosetta Heliocentric distances, the interplanetary magnetic field measured by ACE at 1AU, the Sun-spot number, and the computed tilt angle of the heliospheric current sheet. The peak count rate observed at Rosetta occurs in early 2009 (vertical green line), as the spacecraft passed through the aphelion of one of its orbits around the sun. This peak occurs during the long minimum solar activity and is well correlated with the minimum of interplanetary magnetic field of ~ 4 nT. The HEND peak in late 2009 is coincident with the Rosetta peak, being about at the same heliocentric distance, and the Rosetta count rate is close to the values observed at 1 AU by INTEGRAL and Proba-1. The relative enhancement of the Rosetta count rate in 2010 is coincident with Rosetta's outbound leg, at heliocentric distances of ~ 3.5 AU or more, shortly before rendezvous manoeuvres and hibernation and again could be associated with the radial gradient of GCRs in the inner heliosphere. However, following hibernation exit in 2014, Rosetta's SREM count rates are similar to HEND even though Rosetta is ~ 4.2 AU at this time. Shortly after, surprisingly, the values dropped below the other measurements. This behaviour is discussed in section 3.3.

The count rates from all spacecraft display a ~~long-term~~ long-term variation over ~ 13 years, which we compare with various solar wind parameters. The interplanetary magnetic field (IMF) and Solar wind measured by the Advanced Composition Explorer (ACE) (Stone et al., 1998; Smith et al., 1998; McComas et al., 1998) along with the tilt of the heliospheric current sheet is plotted in the other panels of Figure 4. The heliospheric current sheet (HCS) tilt is the maximum latitudinal extent of the HCS, computed using a potential field model applied to photospheric magnetic field observations (Hoeksema, 1995; Ferreira and Potgieter, 2003), showing the known solar cycle modulation of GCRs. In addition, the expected anticorrelation between GCR and IMF and Sun-spot number was ~~ealeulated-analyzed~~ and the result can be found in Annex 1. This anticorrelation is due to the modulation of GCR intensity. The GCR intensity decreases when the magnetic field and the solar activity increase due to the GCR diffusion in the solar wind. This "engineering" data is a new data set that can be useful to study this modulation.

3.2 Helioradial gradient of cosmic rays

The availability of data from a family of instruments at different heliocentric distances allows the radial gradient of cosmic rays to be examined, providing an insight into the behaviour of the galactic cosmic ray propagation between 1 and 4.5 AU. The cosmic ray radial gradient is computed following the equation (Webber and Lockwood, 1991):

$$Gr = \ln(N_2/N_1) / (r_2 - r_1)$$

(1)

Where N is the count rate and r is the heliocentric radial distance at locations 1 and 2, where $r_2 > r_1$. [Since N are count rates, Gr is an integral gradient.](#)

5

The radial gradient was computed from the INTEGRAL and Rosetta data set for selected periods of the Rosetta mission (e.g. in between planetary flybys), and the results are summarised in Table 3, which contains also some key heliophysics parameters.

Period	Rosetta heliocentric distance [AU]	Solar activity	Range of IMF at 1 AU [nT]	Range of tilt angle [degrees]	Radial gradient [%/AU]
2005-07-01 to 2006-06-30	1.43-1.75	Low	4.39-6.70	9.70-24.10	1.68±0.44
2007-01-01 to 2007-10-31	1.08-1.59	Low	3.91-5.14	11.30-15.90	2.59±0.48
2008-03-01 to 2009-10-31	1.10-2.26	Minimum	3.56-4.34	4.50-17.60	3.16±0.16
2010-01-01 to 2011-06-30	1.13-4.43	Medium	3.95-6.27	17.80-64.10	3.16±0.17
2014-01-01 to 2014-03-17	4.31-4.41	High	4.68-6.98	54.40-70.50	2.13±0.09

10 **Table 3: Radial gradients obtained for a given Rosetta-Sun distance, solar activity, interplanetary magnetic field and computed tilt angle for the mentioned periods. There are no obvious correlations between the radial gradient and the heliophysics parameters.**

Using equation (1) we consider the evolution of the radial gradient between Rosetta and INTEGRAL for the entire mission in Figure 5, where the different coloured points indicate the different phase of the mission. Blue are pre-hibernation data, orange are January-July 2014 and green are July 2014-September 2016 data. A fit has been computed to the pre-hibernation data (red line) and the July 2014-September 2016 data (black line). During the pre-hibernation phase, the slope, which corresponds to the radial gradient, is found to be 2.96 ± 0.12 %/AU. [This positive gradient is mainly due to the inward diffusion of GCRs in an interplanetary magnetic field whose strength decreases with heliocentric distance.](#) This result agrees well with previous studies [for which the energy range can be compared with the TC2 range of ~0.2 – 20 GeV](#) (e.g. Vos and Potgieter, 2016 / [range 0.1-10 GeV](#); Gieseler and Heber, 2016 / [range 0.45-2 GeV](#)). The slope during the comet phase [\(the start of this phase is marked by the red vertical bar on Figure 1b\)](#) was found to be -2.8 ± 0.12 %/AU. In Figure 6, the count rate variation at Rosetta and INTEGRAL are shown. The drop in the count rate occurs during the approach phase, between February and May 2014. After that period [\(green points and black fit\)](#), the count rate variation and the ratio is in very good agreement with the expectation of a positive radial gradient of about 2.9 %/AU (e.g. Vos and Potgieter, 2016; Gieseler and Heber, 2016).

15

20

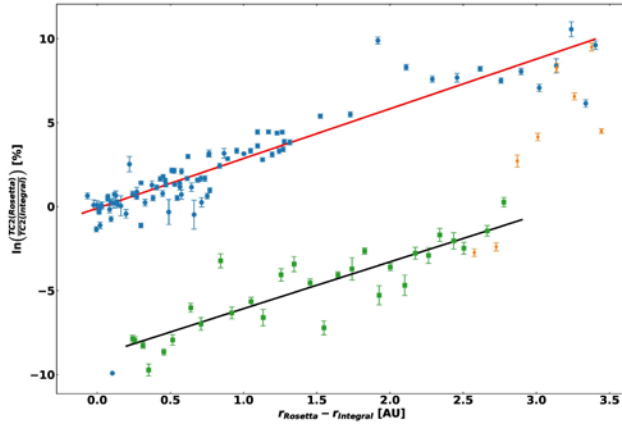


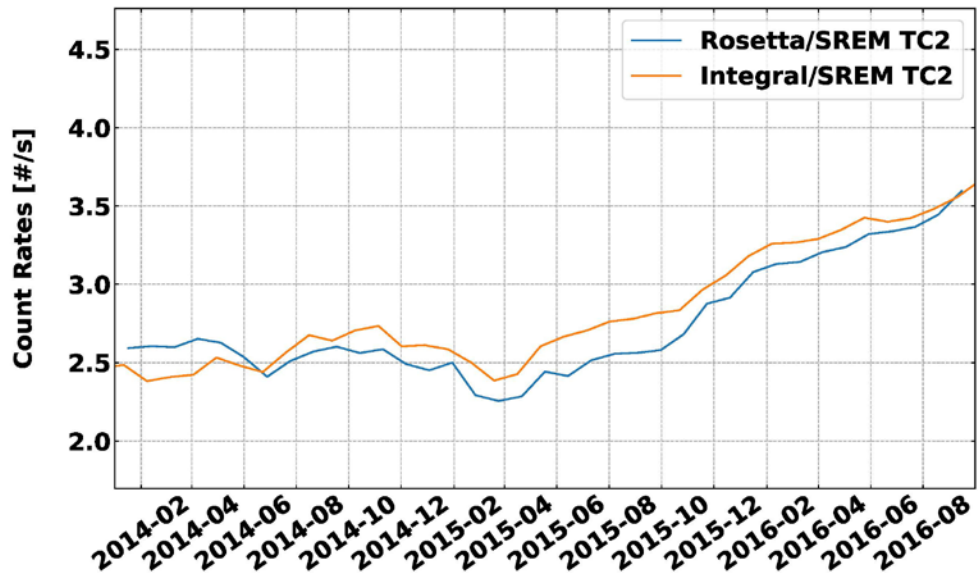
Figure 5: Logarithmic ratio of Rosetta and Integral SREM TC2 data drawn against the difference in heliocentric distance of Rosetta and `INTEGRALIntegral`. The data in blue indicates the time before Rosetta's hibernation mode, the data in orange indicates the time right after hibernation mode until end of July 2014 and the data in green are from August 2014 until the end of the Rosetta mission in September 2016. The performed fits in red and black yield the corresponding radial gradients.

3.3 Apparent attenuation of galactic cosmic ray flux in the vicinity of 67P

This section discusses the relative change in GCR counts at Rosetta compared to INTEGRAL during the comet phase of the mission in 2014. This change of behavior can be observed on Figure 6. The Rosetta counts, initially above INTEGRAL, rapidly decrease and remain below INTEGRAL for the rest of the time period. This change is illustrated in Figure 5 by the ~~dark-black~~ and red fits. A similar behaviour can be observed in all three channels/detectors of SREM. Comparing the two fits (red and ~~dark-black~~ lines), the GCR fluxes after August 2014 are ~8 % lower than expected from the pre- July 2014 data. We note that the count rates at Mars always stay higher than those registered near the Earth (See Figure 4), even during the period shown in Figure 6. This is consistent with a permanent positive GCR radial gradient and supports that the reduction in the GCR rates at Rosetta compared to Earth is related to the comet approach.

Another way in looking at this GCR attenuation during the Rosetta comet phase is to compute the ratio between the measured and the simulated Rosetta SREM TC2 count rate, assuming the calculated radial gradient during the Rosetta cruise phase. The results are displayed on Figure 7. The second panel shows in particular the trend of the attenuation, which reaches a plateau of

-8 % relatively constant during the comet phase. For completeness, the Rosetta heliocentric and the spacecraft-comet distances are shown on the 3rd and 4th panels.



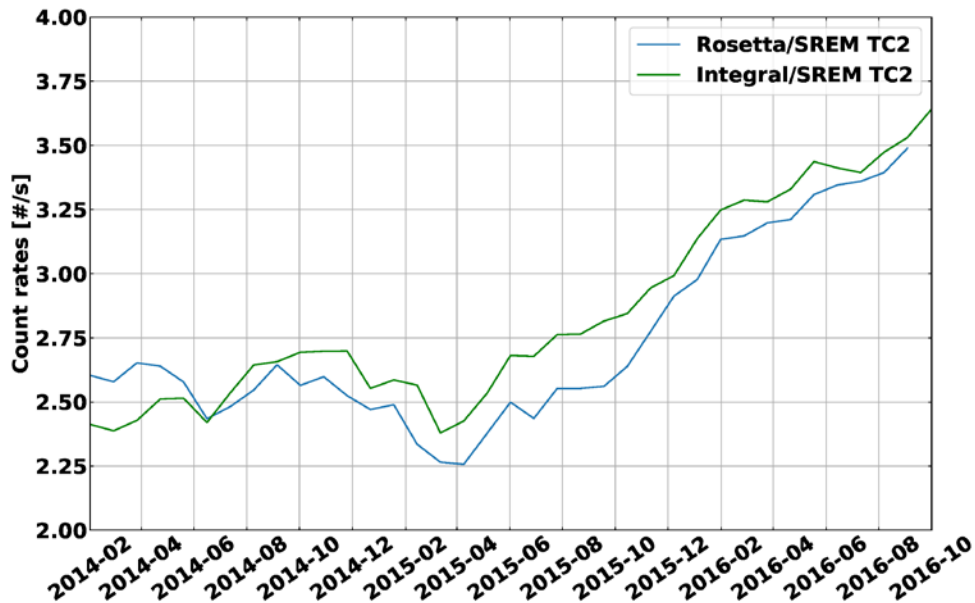


Figure 6: Zoom on the INTEGRAL and Rosetta SREM count rates during the period of the nominal Rosetta scientific mission. The Rosetta data clearly goes below INTEGRAL in spring 2014.

- 5 In order to discuss different reasons for this apparent attenuation, we looked for changes in environmental conditions. The attenuation effect coincides with the overall Solar polarity change (the transition from a A<0 to a A>0 cycle). Previous studies have indicated a dependence of GCR fluxes with Solar polarity (e.g. Potgieter, Burger and Ferreira, 2001) with radial gradients being smaller during A>0 cycles. Negative latitudinal gradients have been reported (e.g. Potgieter, Burger and Ferreira, 2001), but only a fraction of one % per degree (Gieseler and Heber 2016). During the comet phase, Rosetta moved from around -7.5
- 10 ° to +7.5 ° heliolatitude, which could not account for the decrease in GCR fluxes. However, latitudinal gradients have only been reported during A<0 cycles, as opposed to the cycle 24, where A>0.

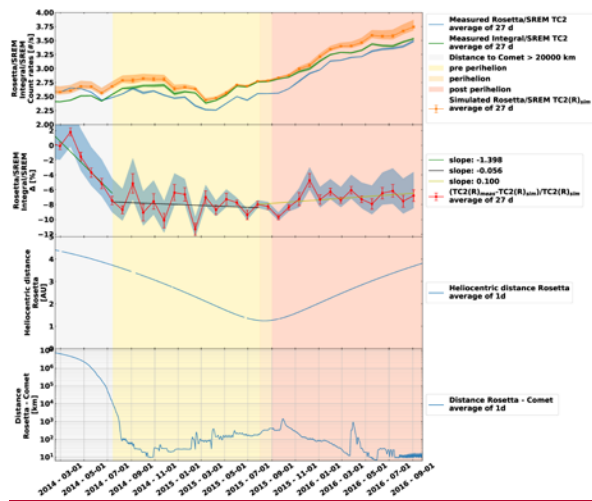


Figure 7: 1st panel: INTEGRAL SREM data, measured and simulated Rosetta SRM data. 2nd panel: Computed GCR absorption. 3rd panel: Rosetta heliocentric distance. 4th panel: Rosetta-nucleus distance. Colours in the background from left to right indicate different stages: when the Rosetta-comet distance was above 20,000 km (grey); pre-perihelion phase (light yellow); perihelion (darker yellow) post-perihelion (light red).

The decreasing ratio begins when Rosetta reaches around 20,000 km from the cometary nucleus and persists more or less at the same level until the end of the Rosetta mission. We cannot discern any anomalous Rosetta SREM instrumentation behaviour during the comet phase. For example, the period May-July 2014 coincided with several large rendezvous manoeuvres, where hundreds of kg of propellant material were used. A similar (in magnitude) series of manoeuvres were also implemented prior to hibernation in early 2011 suggesting thruster induced contamination or deterioration of the SREM detectors is not responsible. In addition, one would not expect the reduction of propellant within the fuel tanks to increase shielding. We note that INTEGRAL count rates are also consistent with Proba-1 measurements during this period, suggesting both instruments are behaving nominally. For completeness, we checked that the separation with the Philae module in November 2014 did not have noticeable effect.

We have considered the solid angle presented by the nucleus to have some impact on counts, with the comet angular size getting as high as 30° in November 2014 during lander delivery and ~ 70° in September 2016. However, a majority of the time the angular size was < 10°, and insignificant (<< 10°) when the “attenuation” began in early 2014, suggesting the nucleus is not a major driver here.

Ground based measurements of the comet indicate cometary activity already began in February 2014 (Snodgrass et al., 2016) with Rosetta remote observations by the OSIRIS camera being able to resolve coma activity in March-April 2014, indicating a coma extent of around 1000 km at that time (Tubiana et al., 2015). However, it was not until August that the in-situ instruments onboard Rosetta began to discern a coma signal, when the spacecraft got to within 100 km of the nucleus (Altwegg et al., 2015; Rotundi et al., 2015) so, the transition in behaviour occurs before the spacecraft is immersed in the cometary coma. Nucleus activity and coma extent increases significantly in the subsequent months (e.g Hansen et al., 2016) yet with no corresponding change in the gradient of GCR over this time. However, the potential shielding of the cometary gas and dust and associated plasma environment cannot be fully ruled out.

4 Discussion and concluding remarks

In this study, we have analysed data from the SREM instruments onboard several ESA spacecraft as well as the HEND instrument onboard Mars Odyssey. The combination of all these different instruments give us multi-point observations of GCR within the Solar System, which constitute a very useful and rich dataset. It is important to note that the primary purpose of this dataset is engineering. However, they are highly valuable for pure scientific studies as illustrated in this paper. Our first step was to calibrate the different SREM sensors onboard different spacecraft, such as ROSETTA, INTEGRAL, HERCHEL, PLANCK, and PROBA-1. Then, the ROSETTA data was also calibrated with respect to HEND on board Mars Odyssey at Mars' distance.

In addition, the data are averaged over ~~a solar rotation period of~~ 27 days, in order to avoid longitudinal effects. However, not doing so allows to study time shifts between solar wind features between Earth and another location, as illustrated in Annex 2.

As a result, we have obtained a very useful dataset, totally calibrated, that give us information of the evolution of GCR with the solar cycle and heliocentric distance evolution. Some additional information regarding the GCR variability with respect to the interplanetary magnetic field (IMF) and sun-spot number (SSN) can be found in the Annex.

We have also demonstrated ~~spacecraft's component material~~ the value of the combination of such data sets in giving a broad view of the distribution of galactic cosmic rays in the inner heliosphere, both geographically spatially and temporally. An important point has been the confirmation of the modulation of galactic cosmic rays with respect to solar activity, as well as the anticorrelation with the interplanetary magnetic field. Also, thanks to the unique Rosetta trajectory within the inner Solar System, the helioradial gradient of galactic cosmic rays between 1 and 4.5 AU was found to be 2.96 %/AU (~~between-2004-10-21 to 2011-05-21~~), matching previous reports (e.g. Vos and Potgeiter, 2016). This information provides insights into the behaviour of the galactic cosmic ray propagation within the inner heliosphere.

When considering the cometary phase of the Rosetta mission, from early 2014 to September 2016, the radial gradient changed, equivalent to an overall 8% attenuation in count rate, and reversed, with count rates at INTEGRAL persistently greater than those at Rosetta, contrary to general expectations. We have considered several potential influences on these measurements to explain this observation, including heliospheric and more local environment conditions. Although several aspects can be discounted for the GCR reduction in the comet environment, further work needs to be carried out on the nature of the overall cometary coma characteristics to quantify its potential impact, along with heliospheric GCR modulation associated with the solar polarity changes. The combination of the extended minimum of Solar cycle 23 with the weakest Solar maximum (cycle 24) for a century, coincident with the time period under scrutiny will also be examined.

10 In addition, other possible follow-up studies include a detailed temporal and spatial analysis of all the radiation datasets, as well as short scale variations of the GCR flux between close points, such as between Earth and Lagrange point L2, or when Rosetta did a flyby to Earth and Mars.

Acknowledgements

15 T. Honig acknowledges the ESA stagiaire program. The authors thank Oldenburg colleagues for useful discussions. The SREM data are available at https://spitfire.estec.esa.int/ODI/dplot_SREM.html. [The sunspot numbers are available at https://spitfire.estec.esa.int/ODI/dplot_ssn.html](https://spitfire.estec.esa.int/ODI/dplot_ssn.html). The HEND data are available at NASA PDS. The ESA Solar proton event archive can be found at: <http://space-env.esa.int/index.php/Solar-Proton-Event-Archive.html>. HCS and Solar polar field data are available at <http://wso.stanford.edu>. Rosetta is an ESA mission with contributions from its member states and NASA. B.S.-
20 C., acknowledges support through STFC grant ST/S000429/1 .

References

- Altwegg, K., et al., 67P/ Churyumov-Gerasimenko, a Jupiter family comet with a high D/H ratio, *Science* Vol. 347, Issue 6220, 2015
- 5 Belov, A., Large scale modulation: view from the earth, *Space Science Reviews* 93: 79-105, 2000
- Ngobeni, M.D., and M.S. Potgieter, The heliospheric modulation of cosmic rays: Effects of a latitude dependent Solar wind termination shock, *Advances in Space research*, 46, 391-401, 2010
- 10 Boynton et al., The Mars Odyssey gamma-ray spectrometer instrument suite, *Space Sci. Rev.*, 110, 37 –83, doi:10.1007/978-0-306-48600-5, 2004
- Cane, H.V. G. Wibberenz, I.G. Richardson and T.T. von Roseninge, Cosmic ray modulation and the Solar magnetic field, *GRL*, Vol. 26, No. 5, 565-568, 1999
- 15 Carslaw, K. S.; Harrison, R. G.; Kirkby, J, Cosmic Rays, Clouds, and Climate, *Science*, Volume 298, Issue 5599, pp. 1732-1737 (2002).
- Evans, H. et al., Results from the ESA SREM monitors and comparison with existing radiation belt models, *Advances in Space Research*, Volume 42, Issue 9, p. 1527-1537, 2008
- 20 Everton F. et al., Effects of solar activity and galactic cosmic ray cycles on the modulation of the annual average temperature at two sites in southern Brazil, *Annales Geophysicae*, Volume 36, Issue 2, 2018, pp.555-564, 2018
- [Glassmeier, K. H., et al., RPC-MAG the fluxgate magnetometer in the ROSETTA plasma consortium, *Space Sci. Rev.*, 128: 649–670, 2007, doi:10.1007/s11214-006-9114-x.](#)
- 25
- Hansen, K.C. et al., Evolution of water production of 67P/ Churyumov-Gerasimenko: an empirical model and multi-instrument study, *MNRAS*, 462, S491-S506, 2016
- Heber, B. and M.S. Potgieter, Galactic and anomalous cosmic rays through the Solar cycle: New insights from Ulysses, in *The Heliosphere through the Solar activity cycle*, edited by Balogh, Lanzerotti and Suess, Springer-Praxis books in astronomy and space sciences, 2008
- 30

Heber, B., J. Kota, and R. von Steiger (2013), Foreword, *Space Sci. Rev.*, 176(1–4), 1–2, doi:10.1007/s11214-013-9998-1.

Hoeksema, J. T., The Large-Scale Structure of the Heliospheric Current Sheet During the ULYSSES Epoch, *Space Science Reviews*, v. 72, p. 137-148, 1995.

5

Ferreira, S.E.S., M.S. Potgieter, Modulation over a 22-year cosmic ray cycle: on the tilt angles of the heliospheric current sheet, *Advances in Space Research*, Vol. 32, No.4 pp.657-662, 2003

Gieseler, J., and B. Heber, Spatial gradients of GCR protons in the inner heliosphere derived from Ulysses COSPIN/KET and PAMELA measurements, *A&A*, 589, A32, 2016

10

Lawrence, D. J., P. N. Peplowski, W. C. Feldman, N. A. Schwadron, and H. E. Spence (2016), Galactic cosmic ray variations in the inner heliosphere from solar distances less than 0.5 AU: Measurements from the MESSENGER Neutron Spectrometer, *J. Geophys. Res. Space Physics*, 121, 7398–7406, doi:10.1002/2016JA022962

Lüdeke, S., Wyrwol, V., "Validation of Flux Models to Characterize the Radiation Environment in Space Based on Current Rosetta-Data", Masters Thesis, Oldenburg, 14 Sept, 2017.

15

Mohammadzadeh et al., The ESA standard radiation environment monitor program: first results from PROBA-I and INTEGRAL, *IEEE Trans. Nucl. Sci.*, vol. 50, no. 6, pp. 2272-2277, Dec. 2003.

Potgieter, M.S., Solar Modulation of Cosmic Rays, *Living reviews of Solar Physics* , 10, 2013, 3

20

McComas, D. J., Bame, S. J., Barker, P., Feldman, W. C., Phillips, J. L., Riley, P., and Griffee, J. W.: Solar wind electron proton alpha monitor (SWEPAM) for the Advanced Composition Explorer, *Space Sci. Rev.*, 86, 561–612, 1998.

Mewaldt, R., Davis, A., Lave, K., Leske, R., Stone, E., Wiedenbeck, M., Binns W., Christian, E., Cummings, A., De Nolfo, G., Israel, M., Labrador, A., Von Rosenvinge T.,: 2010, Record setting cosmic ray intensities in 2009 and 2011, *Astronophys. J. Lett.* 723, L1-L6.

25

Pierce, J., Cosmic rays, aerosols, clouds, and climate: Recent findings from the CLOUD experiment, *Journal of Geophysical Research: Atmospheres*, Volume 122, Issue 15, pp. 8051-8055, 2017

Potgieter, M.S., R.A. Burger, S.E.S. Ferreira, Modulation of cosmic rays in the heliosphere from Solar minimum to maximum: A theoretical perspective, *Space Science Reviews*, 97:295-307, 2001

30

Potgieter, M.S., and E. E. Vos, Difference in the Heliospheric modulation of cosmic-ray protons and electrons during the Solar minimum period of 2006-2009, *A&A*, 601, A23, 2017.

- Rotundi, A., et al., Dust measurements in the coma of comet 67P/Churyumov-Gerasimenko inbound to the sun, *Science* Vol. 347, Issue 6220, 2015
- Sanchez-Cano et al., Mars plasma system response to Solar wind disturbances during Solar minimum, *J. Geophys. Res. Space Physics*, 122, doi:10.1002/2016JA023587, 2017.
- Sánchez – Cano, B., Witasse, O., Lester, M., Rahmati, A., Ambrosi, R., Lillis, R., et al. (2018). Energetic particle showers over Mars from comet C/2013 A1 Siding Spring. *Journal of Geophysical Research: Space Physics*, 123, 8778– 8796. <https://doi.org/10.1029/2018JA025454>
- Smith, C. W., L’Heureux, J., Ness, N. F., Acuña, M. H., Burlaga, L. F., and Scheifele, J.: The ACE Magnetic Fields Experiment, *Space Sci. Rev.*, 86, 613–632, 1998.
- Snodgrass et al, Distant activity of 67P/Churyumov-Gerasimenko in 2014: Ground-based results during the Rosetta pre-landing phase, *A&A*, 588, 2016
- Stone, E. C., Frandsen, A. M., Mewaldt, R. A., Christian, E. R., Margolies, D., Ormes, J. F., and Snow, F.: The Advanced Composition Explorer, *Space Sci. Rev.*, 86, 1–22, 1998.
- Tubiana, C. et al., 67P/Churyumov-Gerasimenko: Activity between March and June 2014 as observed from Rosetta/OSIRIS, *A&A* 573, A62 (2015)
- Utomo, Y.S. Correlation analysis of Solar constant, Solar activity and cosmic ray, *J. Phys.: Conf. Ser.* **817** 012045, 2017
- Vos, E.E., and M.S. Potgieter, Global gradients for cosmic-ray protons in the heliosphere during the Solar minimum of cycle 23/24, *Solar Physics*, 291:2181-2195 (2016)
- Webber, W.R., and J.A. Lockwood, An observation of a heliospheric magnetic cycle dependence for the integral radial gradient of E> 60 MeV cosmic rays, *JGR*, Vol. 96, No. A9, pp 15,899-15,905, Sept 1, 1991
- Witasse, O. et al.: Interplanetary coronal mass ejection observed at STEREO-A, Mars, comet 67P/Churyumov-Gerasimenko, Saturn, and New Horizons en route to Pluto: Comparison of its Forbush decreases at 1.4, 3.1, and 9.9 AU, *J. Geophys. Res. Space Physics*, 122, 7865–7890, doi: 10.1002/2017JA023884, 2017

Zeitlin et al., 2010, Mars Odyssey measurements of galactic cosmic rays and solar particles in Mars orbit, 2002-2008, Space Weather, Volume 8, CiteID S00E06.

Annex 1: Anticorrelation with interplanetary magnetic field and sunspot number

The anticorrelation between radiation monitor count rates and the IMF magnitude and sun-spot number is evident (e.g. Cane et al., 1999, Potgieter, 2013; Mishra and Mishra, 2016 and reference therein), where the peak count rates at all spacecraft are coincident with the beginning of Solar cycle 24 in December 2008. This period overall registered the highest overall GCR flux of the space age (Mewaldt et al., 2010) following one of the longest and deepest solar minimum for over a century. HEND and SREM counts subsequently decreased by around 50% as solar maximum was reached in April 2014. Figure Annex-1 shows this anticorrelation for the Rosetta, ~~and~~ INTEGRAL TC2 and HEND count rates, averaged over a solar rotation period (27 days).

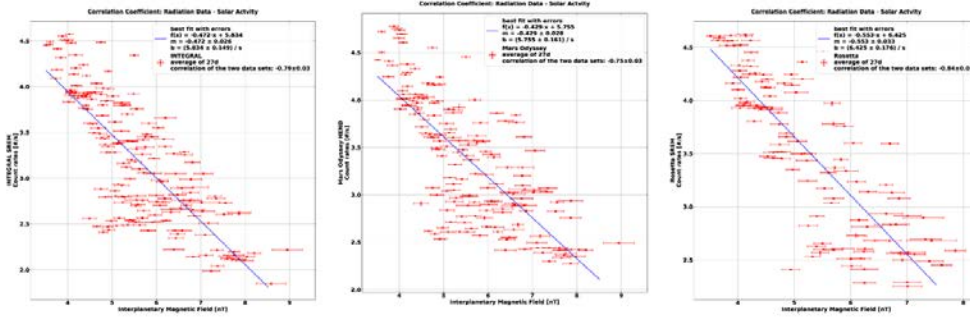
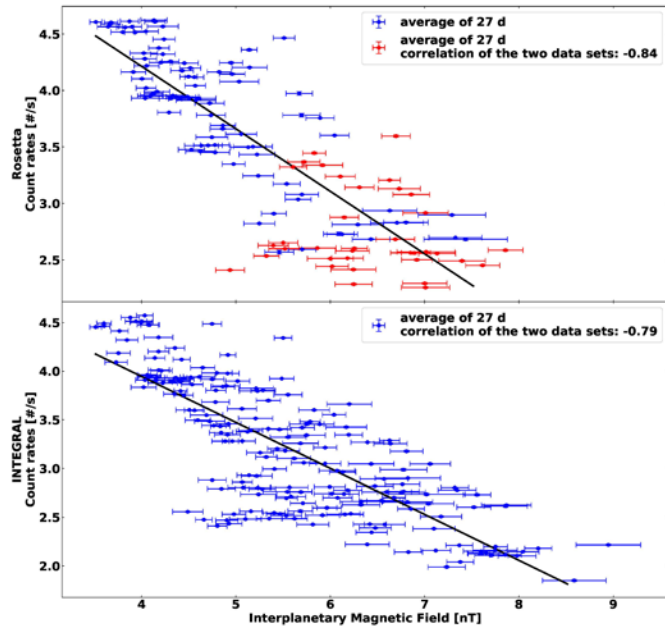


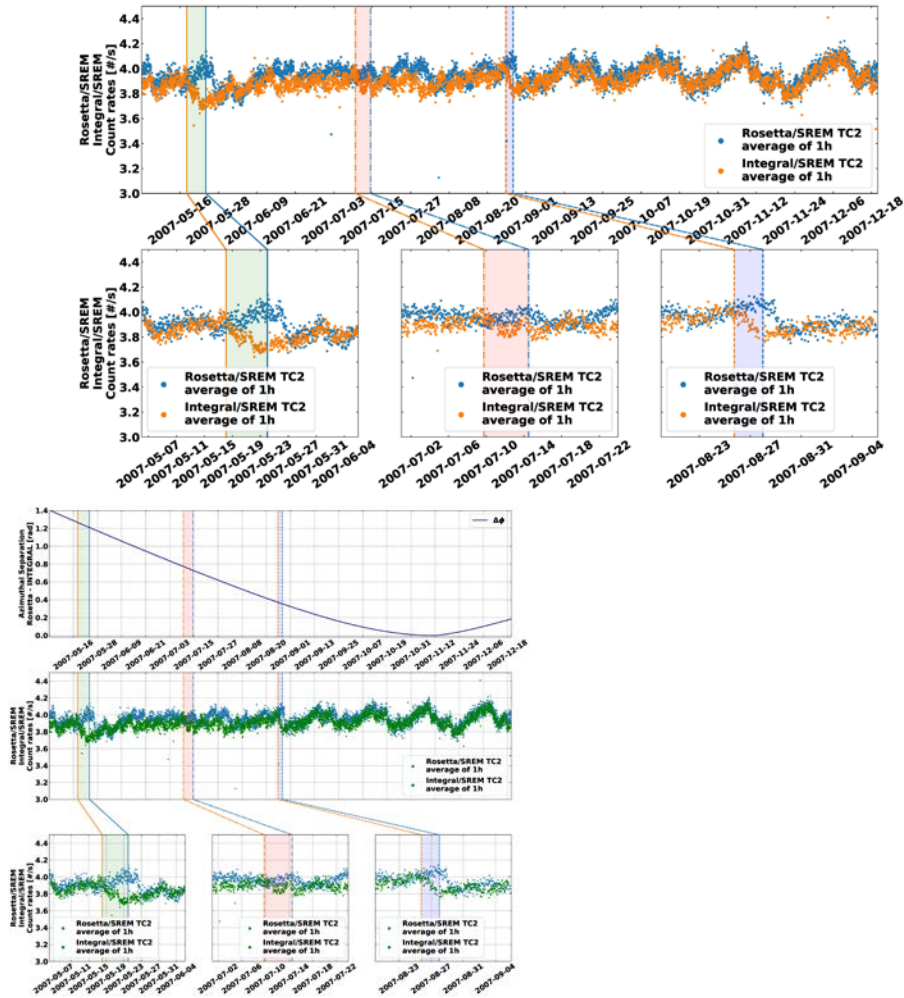
Figure Annex 1: Anticorrelation of Rosetta, HEND and INTEGRAL SREM-radiation data with the IMF. The error bars for all data points correspond to the standard deviation. The Rosetta SREM data in the first panel is distinguished into pre-hibernation phase (blue) and post-hibernation phase (red).

Data set	Rosetta	INTEGRAL	Planck	Herschel	HEND	Proba-1
Period	2004-10-21 to 2016-09-15	2002-10-17 to 20017-02-18	2009-05-14 to 2013-09-23	2009-05-14 to 2013-06-07	2002-01-14 to 2016-06-14	2001-12-10 to 2017-03-30
IMF	-0.84	-0.79	-0.67	-0.73	-0.75	-0.78
SSN	-0.78	-0.67	-0.81	-0.81	-0.77	-0.60

Table Annex -1: Correlation coefficients calculated based on 27 day averaged data from the radiation monitors.

The correlation coefficients, listed in Table Annex-1, show the expected anticorrelation (e.g Cane et al., 1999; Belov et al., 2000 and Utomo, 2017). IMF comparisons have a stronger correlation than the Sun-spot number at Rosetta, Integral and Proba-1 than Planck, Herschel and HEND. Planck and Herschel comparisons are over a shorter time scale during the rising phase of solar cycle 24, and HEND comparisons may be complicated by its indirect measurements of GCRs. Overall, however, the expected trends are well present.

Annex 2: Time shift of solar wind features



5 Figure Annex 2: Solar wind feature shifts. The first panel shows the azimuthal separation between Rosetta and INTEGRAL. The second panel shows the count rates of channel TC2: the count rates of Rosetta SREM TC2 are plotted in blue, while INTEGRAL

SREM data are plotted in green. Both top panels share the same x-axis. First panel: count rates of Rosetta SREM TC2 (blue) and INTEGRAL SREM. The bottom panel displays a zoom of the three periods marked with vertical lines.

TC2 (orange) from May until December 2007. Second panel: Zoom in distributions of the three periods marked with vertical lines.

5

GCR short temporal variations can be driven by coronal mass ejections (CMEs) and corotating interaction regions (CIRs) [e.g. Moraal, 2013; Badrudin and Kumar, 2016; Sanchez-Cano et al., 2017; Witasse et al., 2017] and can influence the timing of signals at various locations in the heliosphere. To demonstrate this, we examine Rosetta and INTEGRAL data during the period from mid until end of 2007. In the first panel of Figure Annex-2, the count rates of channel TC2 of Rosetta (blue) and
10 INTEGRAL (orange) are shown. The temporal delay in the measurement from the two spacecraft is clearly visible and decrease with time. The other panels display a zoomed window of three periods, where correlated features or peaks are indicated in the corresponding data sets by straight, point dashed and dashed vertical lines with INTEGRAL in orange and Rosetta in blue. In May 2007, Rosetta was around 1.58 AU from the Sun and separated in longitude from the Earth by about 60° . In July 2007, Rosetta was around 1.55 AU from the Sun and longitudinally $\sim 45^\circ$ from Earth. Finally, in August 2007, Rosetta was around
15 1.4 AU and only $\sim 15^\circ$ from Earth longitudinally. For the first event, the delay between INTEGRAL and Rosetta is six days and two hours, for the second event, four days and 18 hours and the third event, in August 2007, two days and six hours. These variations are related to the changing relative location/longitude of the spacecraft and Parker spiral configuration. In order to avoid these longitudinal effects, the data are averaged over 27 days (see section 3.1).